AE-293
UDC 539.144.6

AE-293

Absolute M1 and E2 Transition Probabilities in ^{233}U

S. G. Malmskog and M. Höjeberg

AKTIEBOLAGET ATOMENERGI

STOCKHOLM, SWEDEN 1967

ABSOLUTE M1 AND E2 TRANSITION PROBABILITIES IN ^{233}U

Sven G Malmskog and Mats Höjeberg

ABSTRACT

Using the delayed coincidence technique, the following half lives have been determined for different excited states in ^{233}U: $T_{1/2}$ (311.9 keV level) = (1.20 ± 0.15) x 10^{-10} sec, $T_{1/2}$ (340.5 keV level) = (5.2 ± 1.0) x 10^{-11} sec, $T_{1/2}$ (398.6 keV level) = (5.5 ± 2.0) x 10^{-11} sec and $T_{1/2}$ (415.8 keV level) < 3 x 10^{-11} sec. From these half life determinations, together with earlier known electron intensities and conversion coefficients, 22 reduced B(M1) and B(E2) transition probabilities (including 9 limits) have been deduced. The rotational transitions give information on the parameters δ and $(g_K - g_R)$. The experimental M1 and E2 transition rates between members of different bands have been analysed in terms of the predictions of the Nilsson model, taking also pairing correlations and Coriolis coupling effects into account.

Printed and distributed in August 1967.

LIST OF CONTENTS

1. INTRODUCTION

Low-lying energy levels in ^{233}U are populated in the β^- decay of ^{233}Pa ($T_{1/2}$ = 27 days). Recent high-resolution electron energy and intensity measurements have been reported by Albridge et al. [1], Schultze and Ahlf [2] and Bisgård et al. [3], while only Albridge et al. report on a direct measurement of the gamma ray intensities. The above information has been used by these authors to determine multipolarities and mixing ratios for the observed transitions. A consistent decay scheme of ^{233}U has then been proposed, including Nilsson orbital assignments for the different levels.

In the present investigation we have measured the gamma ray intensities in the decay of ^{233}Pa with a Ge(Li) detector and the half lives of excited states in ^{233}U using the delayed coincidence technique. This new information, together with earlier known electron intensities and total conversion coefficients [4], has made it possible to deduce 22 reduced B(M1) and B(E2) transition probabilities (including 9 limits). These B(M1) and B(E2) values have been divided into six different groups according to the multipolarity of the transition and the difference of the K-quantum number of the initial and final states of the pertinent transition. Each group has separately been analysed within the Nilsson model [5] taking also pairing correlations [6] and Coriolis coupling [7, 8] effects into account.

2. EXPERIMENTAL PROCEDURES

2.1 Source preparation

Spectroscopically pure thorium oxide was irradiated for three days in a thermal neutron flux of 3×10^{13} n/cm^2 sec. in the reactor R2 at Studsvik. ^{233}Th, which was produced by the ^{232}Th (n, γ) reaction, decays by β emission with a half life of 23.5 min. to ^{233}Pa. To get rid of the high ^{233}Th activity the irradiated container was allowed to decay for one week before being handled. Thin sources for the coincidence measurements using the low energy electrons in ^{233}U were needed. Therefore a solution of the irradiated material was put onto an ion ex-

change column which separated out the Pa isotope, which was put on to a thin VYNS backing, furnacad with a thin gold layer, in order to make it electrically conducting. Several sources with different strengths were prepared. The source diameters varied between 3 mm and 5 mm.

For comparison purposes we used in some of the half life determinations the β→239 K cascade in the decay of ^{212}Pb (Th-B). This source was prepared in the following way. A very thin aluminium foil was spanned on a nylon ring and placed in a closed chamber together with a ^{228}Th source, which gives the thorium 4n series in equilibrium. A high tension of 500 V made the activity stick to the aluminium foil. The intermediate products are very short lived and thus we only get a thin ^{212}Pb source ($T_{1/2}$ = 10.6 h).

2.2 Gamma ray measurement

We have recorded the gamma ray spectrum with a 5 mm thick Ge(Li) detector supplied with a cooled FET pre-amplifier. This system had an energy resolution (FWHM) of 1.8 keV at 250 keV. All the gamma rays above approximately 50 keV reported by Albridge et al. (table 2 of ref. [1]) were also observed by us. Our gamma ray intensities are in general agreement with those of Albridge et al. We also observed a weak new line corresponding to the energy 248.69 ± 0.24 keV and with an intensity of 0.05 ± 0.02 per cent per beta decay (the same normalization as that used by Albridge et al.). For energy reasons we consider this gamma ray to be the 5/2 $3/2^+ \rightarrow 9/2$ $5/2^+$ transition .

2.3 Instrumentation for the half life measurements

The basic instrument for the half life measurements to be described has been a long lens electron-electron coincidence spectrometer similar to the one earlier described by Gerholm and Lindskog [9]. To obtain a good energy and time resolution, we have used electron detectors with light guides of a special shape [10] which are furnished with conically shaped Naton 136 plastic scintillators. These electron detectors are optically coupled to the photomultiplier 56 AVP. The measured time dif-

ference pulses are taken from a time-to-pulse heitht converter and registered on a multichannel analyser. The linearity, stability and time calibration of this system were checked several times during the measurements using an air core delay line similar to the one described by Graham et al. [11].

For greater convenience in the centroid shift measurements using the comparison method on longer lived activities, the source holder can be furnished simultaneously with two active sources placed 27.5 cm apart. This holder can then, at pre-set times, be shifted automatically between two positions without breaking the high vacuum, which allows measurements on either of the two sources. This source holder is also made of an insulating material (PVC rod) which makes it possible to apply a high tension of at least 30 kV to the source. In the case of a self comparison measurement it is also possible to automatically change between measurements with and without high tension. Details of the electronic system have been given earlier [12].

2.4 Experimental methods

The half lives measured in this work have been obtained using the centroid shift technique either as a comparison measurement with two different sources or as a self comparison measurement with only one source. In both types of measurement coincidences from electron-electron cascades have been registered in the double lens spectrometer.

In the first case the unknown half life was determined from the centroid shift produced from the mean life of the actual level where a prompt ($\leq$1 psec delay of intermediate level) $\beta\rightarrow$ conversion electron cascade from a ^{212}Pb (Th-B) source was used to define a zero time. The observed time shift then corresponds to the mean life of the intermediate level being studied [13]. Such a statement is only true, however, if energy-dependent instrumental time shifts can be neglected and this is generally not the case when the half lives of the levels under investigation are of the order of or less than 10^{-10} sec. These shifts are mainly due to the energy-dependent response of the detector and the variation of transit time of the electrons through the spectrometer with electron energy. To avoid the uncertainties

from corrections for these energy effects the best thing in all types of comparison measurements is to have fixed energy settings throughout the whole measurement. This can be achieved, for instance, by finding a suitable comparison source with a sufficiently high energetic β-branch which feeds a level which decays with a conversion electron line equal in energy with one line in the actual cascade. This requirement is usually not easy to fulfil, especially as the intermediate level in this comparison source must also have an accurately known half life or be known to have a half life much smaller than the level being studied. Another possibility is to compensate for the electron energy difference in the two sources. We have made such a compensation possible by providing our spectrometer with an insulated source holder so that the electrons can be accelerated or retarded by applying a negative or a positive potential to the active source relative to the spectrometer itself. A correction for the finite accelaration time has then to be applied. This term is of the order of < 10 psec for electron energies >20 keV.

In the self-comparison measurement only one cascade of transitions is involved. One time distribution is obtained when coincidences between the two transitions in a cascade are registered and another one when these transitions are detected in the opposite detectors. The centroid shift between two such time distributions corresponds to twice the mean life of the intermediate level [13]. Using this method we also have to correct for the energy-dependent instrumental time shifts or to compensate for the energy difference as mentioned above.

In the case of ^{233}U some of the β→electron cascades are very suitable for making a self-comparison measurement. In these cases the feeding β branches have maximum energies which are roughly 2-3 times the energy of the pertinent de-exciting conversion line. The first time distribution is registered with one lens focussed on the conversion line while the other lens is set on the β continuum slightly above this line. After the application of a proper negative high-tension to the source the electron line will be focussed in the second lens while the first

lens will detect β particles with energies just below the relevant line. As the energy settings have been kept at a fixed value during this procedure the energy dependent contributions mentioned earlier will be negligible. Corrections have to be applied for the finite acceleration distance and for unwanted coincidence contributions. Such corrections have to be deduced for each separate measurement taking electron energy and intensity data as well as spectrometer resolution effects into account.

2.5 Half life measurements

^{233}Pa decays mainly by four roughly equally intense β^- branches to the members of the $3/2^+$ and $1/2^+$ rotational bands in ^{233}U. An electron spectrum, taken with one lens set to 3 % relative momentum resolution, is shown in fig. 1. Comparison (two sources) as well as self comparison (one source) measurements have been performed in order to determine half lives of the excited levels in ^{233}U. As the individual conversion electron lines are not fully resolved from each other, and furthermore due to the unavoidable β continuum under these lines, false coincidence contributions will usually be registered. It is therefore of importance to choose suitable energy settings so as to reduce the influence from such undesirable cascades. In this section a brief description of the relevant choice of energy settings is given for each of the different coincidence measurements together with the centroid shifts observed and a discussion regarding the pertinent corrections. The analysis of the data obtained is postponed to section 3.

415.8 keV level. In this case a self-comparison measurement has been performed utilizing the 75.3 and 103.9 keV transitions from the 415.8 keV level together with the feeding β continuum. In the first run lens number one was focussed on the 75.3 L line while the other lens was set just below the 103.9 M line. With these energy settings only a small correction to the measured coincidence rate from the 86.6 L tail →β has to be applied.

In the second run a high tension of 10 kV was applied to the source. This was just enough to focus the 103.9 L line in the

second lens. The first lens will then automatically be focussed on the β continuum below the 75.3 L line. The main coincidence contributions in this case will come from the β→ 103.9 L, 75.3 L tail →β and β→ 86.6 M cascades.

In order to reduce the influence from long term electronic instability drifts in the centroid position of the measured decay curves, each run was composed of several pairs of measurements, Such a pair consists of one measurement with and one without high tension, each of about 20 minutes' duration. Several runs were performed, usually for 8 - 15 hour periods, using the automatic procedure described in section 2.3. All the data were then analyzed according to the centroid shift method [13]. As a mean value we obtained a centroid shift of 64 ± 23 psec.

398.6 keV level. A self-comparison measurement has been performed using the 86.6 L line and the feeding β continuum. The energy settings were chosen so that the first lens focussed the 86.6 L electrons. To get the energy setting of the other lens, an increasing high tension was applied to the source until the first lens focussed electrons with energies just above that of the high energy side of the 75.3 L line. Keeping this applied voltage of 6 kV the second lens was adjusted to focus the 86.6 L line (see fig. 1). With these energy settings the main coincidence contributions in a run without high tension will come from the 86.6 L →β and β→ 75.3 M cascades. In a similar run with high tension the main contributions will be obtained from the β→ 86.6 L and the 86.6 L tail →β cascades. In each 8 - 15 hour period several pairs of measurements were made in the same way as described above for the 415.8 keV level. The analysis of the data [13] gave as a mean value a centroid shift of 125 ± 30 psec.

We wish to point out that the 86.6 L →β and 86.6 M →β cascades proceed both via the 398.6 keV and the 415.8 keV levels. These cascades will then in addition to the half life of the 398.6 keV level also introduce the half life of the 415.8 keV level into the analysis.

340.5 keV level. In this case a comparison measurement with

the two sources ^{233}Pa and ^{212}Pb has been performed. The first lens focussed the 340.5 K line while the second lens was adjusted to focus electrons with an energy of 148.1 keV (the 239 K line from a ^{212}Pb (Th-B) source with a half life of 10.6 hours). The first measurement essentially gives the $\beta\rightarrow$ 340.5 K time distribution. The small contributions from the 311.9 K tail $\rightarrow\beta$ cascade and the $\beta\rightarrow$ 340.5 K cascade via the 415.8 keV level can be neglected (less than three percent). In the comparison measurement we obtained a prompt time destribution (mean life of intermediate level less than 1 psec.) from the 239 K $\rightarrow\beta$ cascade using the same energy settings. The two sources were both placed on the source holder rod which was automatically shifted between the two measuring positions at 20-minute intervals. Several runs during a period of 6 - 8 hours duration were made. From the analysis of the time distribution data [13] a centroid shift of 75 ± 14 psec was obtained.

311.9 keV level. A self comparison measurement has been performed using the 311.9 K$\rightleftarrows\beta$ cascade. In the first measurement one lens was adjusten to focus the 311.9 K line while the other lens was set to accept β particles with 11.7 keV higher energy. In the next measurement enough high tension was applied to the source to focus the 311.9 K line in the second lens. The first lens will then automatically be focussed on the 311.9 K low energy tail at the position of the 300.2 K line. These energy settings were primarily chosen because of the better accuracy when correcting for the influence from the 300.2 K $\rightarrow\beta$ cascade.

In the first run the main coincidence contribution will be obtained from the 311.9 K $\rightarrow\beta$ cascade both via the 311.9 and 340.5 keV levels. After the application of high tension the main contribution will come from the $\beta\rightarrow$ 311.9 K, 311.9 K tail $\rightarrow\beta$ and 300.2 K $\rightarrow\beta$ cascades. All contributing cascades via the K = 1/2 rotational band members will have no influence, as the populating β particle energies are too low to be registered with the energy settings chosen.

Several 20-minute measurements with and without high tension were registered using the automatic performance of the

equipment. The total time for each measuring period was between 8 - 15 hours. All the data were analysed according to the centroid shift method [13]. As a mean value we obtained centroid shift of 310 ± 35 psec.

3. HANDLING OF THE PERTINENT DATA

As indicated in section 2.5 most of the measured time distributions were composed of contributions from more than one cascade. The measured centroid shift will therefore as a rule be a function of two mean lives of intermediate levels in the pertinent cascades. The analytical expressions for these functions have been deduced using the measured electron intensities of Albridge et al. [1], theoretical conversion coefficients [4] and theoretical shapes for the continuous β spectra [14]. The following expressions have been obtained after inclusion of a small correction for the influence from the finite electron acceleration distance

$$(1.52 \pm 0.05)\tau_{415.8} + (0.50 \pm 0.05)\tau_{398.6} = 64 \pm 23 \quad (1)$$

$$(1.53 \pm 0.07)\tau_{398.6} + (0.30 \pm 0.09)\tau_{415.8} = 125 \pm 30 \quad (2)$$

$$\tau_{340.5} = 75 \pm 14 \quad (3)$$

$$(1.71 \pm 0.04)\tau_{311.9} + (0.22 \pm 0.03)\tau_{340.5} = 310 \pm 35 \quad (4)$$

The mean lives τ are here given in psec. The errors have been estimated from the experimental uncertainties in the pertinent intensity branching ratios and spectrometer efficiencies. The following half lives have been obtained from eqs. 1-4.

$T_{1/2}$(415.8 keV level) $\leq$ 30 psec

$T_{1/2}$(398.6 keV level) = 55 ± 20 psec

$T_{1/2}$(340.5 keV level) = 52 ± 10 psec

$T_{1/2}$(311.9 keV level) = 120 ± 15 psec

where the statistical errors have been given. The half life of the 311.9 keV level has been reported earlier as (200 ± 30) psec [15] and < 100 psec [16]. All the pertinent experimental data required

for the following discussion have been compiled in table 1. The electron intensities and E2/M1 mixing ratios from three different investigations [1, 2, 3] have been considered. The partial gamma ray transition probabilities have in most cases been deduced from the electron data and theoretical conversion coefficients. These values usually differ only slightly from those obtained more directly from gamma ray intensity measurements. The reduced B(M1) and B(E2) transition probabilities have been deduced using the electron intensity data of each of the investigations ref. 1-3 and the following formulas

$$B(M1)\downarrow = \frac{3.94 \times 10^{-5}\, N_\gamma(M1)\, E_\gamma^{-3}}{T_{1/2}(\text{level})\, \Sigma\, N_i} \left(\frac{e\hbar}{2Mc}\right)^2 \qquad (5)$$

$$B(E2)\downarrow = \frac{56.4\, N_\gamma(E2)\, E_\gamma^{-5}}{T_{1/2}(\text{level})\, \Sigma\, N_i}\, e^2 b^2 \qquad (6)$$

where $T_{1/2}(\text{level})$ is in sec., E_γ in keV and $\Sigma\, N_i$ denotes the sum of all transition intensities de-exciting the pertinent level. N_γ is the partial gamma ray transition probability for the pertinent transition. In cases of reasonable agreement between the different electron intensity investigations average values adopted for the comparison with theoretical expectations have also been given.

4. DISCUSSION

It is of interest to compare the experimentally observed transition rates with theoretical predictions. A convenient way of presenting the result from such a comparison is to give the hindrance factor, F, for the transition, defined as the theoretically calculated reduced transition probability divided by the corresponding experimental value.

For a rough classification of the data it is suitable to use a simple single-particle estimate [14], although it is well known that such estimates are too crude to be able to take any details into account. The resulting F_W-factors from such a comparison are given in table 1. We can see that the M1 transitions are hin-

dered between 10 to 1000 times. The E2 transition rates within a band are typically enhanced by a factor of 200 while E2 transition rates between different bands have roughly the single-particle strength. Hindrance factors of this size are expected from systematics [21]. The 75.3 and 103.9 keV E2 transition rates do not follow this simple intensity scheme, being enhanced by more than a factor of 25.

A more adequate nuclear model with which to compare the experimental data in the deformed mass regions is the one formulated by Nilsson. According to this model the reduced E2 and M1 transition probabilities can be written [5]

$$B(E2)\downarrow = 1.52 \times 10^{-3} \left[\langle I_i K_i\, 2,\ K_f - K_i \mid I_f K_f \rangle + b_{E2} (-1)^{I_f + K_f} \langle I_i K_i\, 2,\ -K_f - K_i \mid I_f,\ -K_f \rangle \right]^2 G_{E2}^2 \quad (7)$$

$$B(M1)\downarrow = 5.91 \times 10^{-2} \left[\langle I_i K_i\, 1,\ K_f - K_i \mid I_f K_f \rangle + b_{M1} (-1)^{I_f + K_f} \langle I_i K_i\, 1,\ -K_f - K_i \mid I_f,\ -K_f \rangle \right]^2 G_{M1}^2 \quad (8)$$

where $B(E2)\downarrow$ is given in units of e^2b^2 and $B(M1)\downarrow$ in nuclear magnetons. The quanities G_{E2}, b_{E2}, G_{M1} and b_{M1}, which depend on the wave functions of the initial and final states, are defined by eqs. (35) and (36) in ref. [5]. We have used eqs. (7) and (8) to calculate the hindrance factors F_N. To obtain G_{E2} and b_{E2} we have used the potential parameters $\varkappa = 0.05$ and $\mu = 0.45$ with a deformation fixed at $\delta = 0.2$, while for G_{M1} and b_{M1} we have furthermore set $g_R = 0.3$ and $g_s(\text{eff}) = g_s(\text{free}) = -3.826$. The result of this calculation is given in table 1, column 15.

The presence of pairing correlations modifies the calculated transition rates. This modification can be expressed by a pairing factor, $P \leq 1$, with which to multiply the earlier defined G-factors. We have [6]

$$P_\tau = (U_f U_i + \tau V_f V_i)^2 R \quad (9)$$

where U and V are the probability amplitudes for the relevant state to be unoccupied and occupied, respectively, by a pair of particles, $\tau = +1$ for magnetic multipoles and $\tau = -1$ for electric multipoles, and R is a factor close to one. For levels near the Fermi surface where U^2 and V^2 are ≈ 0.5, electric multipole transitions can be strongly hindered as a consequence of the pairing correlations. In the deformed mass regions this possible strong influence, especially on the E2 transition rates, from the pairing correlations is often counterbalanced by the Coriolis coupling [8], causing collective E2 contributions to occur also in interband transitions. In the more detailed discussion to follow, the effects of pairing correlations and Coriolis mixing are considered. In this connection we want to point out that we have consequently used the theoretical predictions of the relevant quantities G_{M1}, b_{M1}, G_{E2} and b_{E2} as well as the Coriolis matrix elements $\langle K_i \mid j_\pm \mid K_f \rangle$ obtained with the potential parameter values recommended by Nilsson [5] ($\varkappa = 0.05$ and $\mu = 0.45$ for N = 6). In the case of asymptotically allowed matrix elements, the predicted values can be regarded as reliable, but in cases of asymptotically forbidden matrix elements this procedure is questionable, especially as we have had no opportunity to investigate the variation of the predicted quantities with the potential parameters $\varkappa$ and μ. To circumvent this problem, at least to a certain extent, we have tried wherever possible, to evaluate the uncertain quantities from experiment and then compared the result with predicted values.

4.1 E2 transition rates within bands

From the experimental value of $B(E2)\downarrow$ for a transition between the $I_i \rightarrow I_f$ spin members of a rotational band, the intrinsic quadrupole moment Q_o can be calculated from the following equation [17]

$$B(E2)\downarrow = \frac{5\,e^2}{16\pi} \langle I_i\, K20 \mid I_f\, K \rangle^2 (Q_o + 2\beta^2 G_{E2}^{s.p.})^2 \qquad (10)$$

where $\beta = \sqrt{\frac{\hbar}{MW_o}}$ which for ^{233}U gives $2\beta^2 = 0.104$ barns. The additional term occurring for K = 1/2 bands can be neglected since the collective contribution to the E2 rate dominates over the single particle contribution. When Q_o is known the deformation parameter δ can be estimated according to the formula [17]

$$Q_o \approx 0.8\ Z\ R_o^2\ \delta\ (1 + 0.5\delta) \qquad (11)$$

where R_o is taken to be $1.2\ A^{1/3}$ fm and Q_o is given in cm^2.

The K = 5/2-band. The intrinsic quadrupole moment Q_o for this band has been determined both in a resonance absorption measurement (Q_o = 9.6 barns) [18] and from a Coulomb excitation measurement (Q_o = 13.7 barns) [19]. The values deduced for the deformation parameter are δ = 0.22 and δ = 0.30 we adopt as an average value $\delta = 0.26 \pm 0.04$.

The K = 3/2-band. The only known rotational transition in this band is the 28.5 keV transition between the $5/2^+$ and $3/2^+$ members. As is seen from eq. (6), the B(E2) value is determined by the energy of the transition, the half life of the initial level, the total transition intensity from that level, and the partial E2 gamma ray intensity for the rotational transition (meaning in this case the total conversion coefficient together with the E2/M1 ratio). The latter quantity has been deduced using the E2 percentage given by each of the three groups mentioned earlier [1, 2, 3], and the corresponding total conversion coefficients obtained from the tables of Rose with the inclusion of an empirical correction for the screening effect [20]. The contribution from the N, O etc. shells has been taken to be $0.3\ \alpha_M$. The resulting B(E2)↓ values are given in table 1. The corresponding deformation parameter values are obtained from eqs. (10) and (11) as δ = 0.18 [1], δ = 0.13 [2] and δ = 0.16 [3], and we adopt a mean value of $\delta = 0.16 \pm 0.03$.

The K = 1/2-band. A 17.3 keV transition between the $3/2^+$ and $1/2^+$ members of this band has been observed, but only one determination of its E2 content (8 ± 5 % E2) has been reported [2]. In this case an upper limit for the half life of the $3/2^+$ 415.8 keV level has been determined which only makes it possible to set a

lower limit for the deformation parameter. This value has been deduced using also a lower limit of 3 % E2 admixture and the corresponding total conversion coefficient $\alpha = \alpha_{L\,III} + 1.3\,\alpha_M$ obtained from Rose [4] including a screening correction [20]. We then obtain $\delta > 0.31$, which is a rather large value. We must, however, keep in mind that this estimate is crude as the result is extremely sensitive to the value of the E2 admixture, especially as a result of its influence on the total conversion coefficient. It may, however, indicate that the E2 admixture of (8 ± ± 5) % as given by Schultze and Ahlf is a little too high.

4.2 E2 transitions with $|\Delta K| = 1$

It has been shown earlier [21] that E2, $|\Delta K| = 1$ transitions are generally strongly enhanced (10^2 - 10^5 times) relative to the Nilsson model. This is also the case for the five E2 transitions observed between the K = 3/2 and K = 5/2 bands, as well as the three E2 transitions between the K = 1/2 and K = 3/2 bands in ^{233}U (see table 1). This enhancement is understood when the mixing of the intrinsic states is taken into account. Specifically the Coriolis mixing between the two intrinsic states involved in the pertinent gamma-ray transition is of great importance since contributions proceeding via collective E2 matrix elements will occur. Faessler [22] has made a calculation of the E2, $|\Delta K| = 1$ transition rates employing a rotating and vibrating core with rotational and vibrational interactions. When an odd particle moves in such a potential, coupling terms of the rotation-particle, vibration-particle, rotation-vibration and rotation-vibration-particle types will occur, which all cause mixing of intrinsic states. The most important effect is expected to come from the rotation-particle term, although mixing with the β- and γ-vibrational bands will in some cases of E2 transitions also be of importance. In the present case we shall only consider the contribution to the E2-transition rate from the important rotation-particle coupling term. The E2 transition rates between the K = 3/2 and K = 5/2 as well as those between the K = 1/2 and K = 3/2 bands will be discussed separately.

$K = 3/2 \rightarrow K = 5/2$ E2 transitions. The reduced E2 transition probability between the bands built on the $3/2^+(631)$ and $5/2^+(633)$ orbitals can be written

$$B(E2, I_i \tfrac{3}{2} \rightarrow I_f \tfrac{5}{2}) = 1.52 \times 10^{-3} \Big[P_-(\tfrac{3}{2} \rightarrow \tfrac{5}{2})\, G_{E2}(\tfrac{3}{2} \rightarrow \tfrac{5}{2}) \times$$

$$\times \langle I_i \tfrac{3}{2}\, 2\, 1 \mid I_f \tfrac{5}{2} \rangle + C(I_f \tfrac{3}{2} \tfrac{5}{2}) G_{E2}^{coll} \langle I_i \tfrac{3}{2}\, 2\, 0 \mid I_f \tfrac{3}{2} \rangle +$$

$$+ C(I_i \tfrac{5}{2} \tfrac{3}{2}) G_{E2}^{coll} \langle I_i \tfrac{5}{2}\, 2\, 0 \mid I_f \tfrac{5}{2} \rangle + C(I_i \tfrac{1}{2} \tfrac{3}{2})\, P_-(\tfrac{1}{2} \rightarrow \tfrac{3}{2}) \times$$

$$\times G_{E2}(\tfrac{1}{2} \rightarrow \tfrac{5}{2}) \langle I_i \tfrac{1}{2}\, 2\, 2 \mid I_f \tfrac{5}{2} \rangle \Big]^2 e^2 b^2 \qquad (12)$$

where higher order terms in the amplitudes C have been neglected. Furthermore, P_- is the pairing factor (eq. 9) and $C\,(I_\nu K_c K_m)$ the amplitude of the wave function for the state $I_\nu K_c$ being Coriolis admixed into the main K_m band. In the perturbation approximation these amplitudes are given by

$$C\,(I_\nu K_c K_m) = -\,E^{\mathcal{H}} \cdot \frac{P_+ \langle K_c \mid j_+ \mid K_m \rangle \sqrt{(I_\nu - K_<)(I_\nu + K_< + 1)}}{E\,(I_\nu K_m) - E(I_\nu K_c)} \qquad (13)$$

$K_<$ being the smallest of K_c and K_m, I_ν the spin of the mixing states, $E^{\mathcal{H}}$ the non-diagonal equivalent to the rotational parameter $\frac{\hbar^2}{2\mathcal{J}}$, and the denominator the estimated energy difference between the two levels being admixed. We also have [8]

$$G_{E2}^{coll} = \frac{1}{2\beta^2}\, Q_o + G_{E2}^{s.p.} \qquad (14)$$

In a first attemp to evaluate eq. (12) we used $P_\pm = 1$, $Q_o = 10$ barns and $E^{\mathcal{H}} = 6$ keV while the G_{E2} and $\langle K_c \mid j_+ \mid K_m \rangle$ values were calculated from the Nilsson model. It then became clear that the terms involving the collective G_{E2}^{coll} factor were quite dominating, which will be further stressed since actually $P_- < 1$. The Coriolis matrix element mixing the $K = 3/2$ and $K = 5/2$ bands is, however, asymptotically forbidden which makes its evaluation from

the model uncertain. We therefore prefer to regard the product of E^{*}, $\langle K_c \mid j_{+} \mid K_m \rangle$ and Q_o ($G_{E2}^{s.p.}$ in eq. (14) can be neglected) as an unknown quantity which will be determined from the relevant experimental B(E2) values. The result is given in table 2.

The intrinsic quadrupole moment Q_o has been measured for the K = 5/2 band in a Coulomb excitation experiment as Q_o = = 13.7 ± 1.9 b [19] and from a resonance absorption experiment as Q_o = 9.6 b [18]. From our half life measurement of the 340.5 keV level and available conversion electron data we get Q_o = 7.0 ± ± 1.5 b for the K = 3/2 band. Furthermore does Sobiczewski [23] give measured values of Q_o for ^{232}U and ^{234}U which are both very close to 10 b. We therefore consider Q_o = (10 ± 3) b to be a reasonable estimate.

We also expect E^{*}, involved in the coupling between low-lying bands to be approximately equal to the rotational parameter $\hbar^2/2\mathcal{J}$ [24], which turns out to be 5.76 keV and 5.70 keV for the K = 5/2 and K = 3/2 bands, respectively. It thus seems reasonable to choose E^{*} = 5.7 keV.

With these estimates of Q_o and E^{*}, we can deduce a value of the Coriolis coupling matrix element $\langle \frac{3}{2} \mid j_{-} \mid \frac{5}{2} \rangle$ from the experimental B(E2) values given in table 2. The result is given in column 6 in the same table and should be compared with the predictions of the Nilsson model giving $\langle \frac{3}{2} \mid j_{-} \mid \frac{5}{2} \rangle$ = 1.40 and 1.08 for δ = 0.2 and δ = 0.3 respectively. These values are calculated with the specific set of potential parameters $\varkappa$ and μ given by Nilsson. Comparison with experiment indicates that the model, at least for the chosen set of $\varkappa$ and μ, overestimates the asymptotically forbidden Coriolis matrix element $\langle \frac{3}{2} \mid j_{-} \mid \frac{5}{2} \rangle$ by roughly a factor of 3.

<u>K = 1/2→K = 3/2 E2 transitions.</u> The reduced E2 transition probability between the bands built on the $1/2^{+}(631)$ and $3/2^{+}(631)$ orbitals can be written

$$B(E2,\ I_i\,\tfrac{1}{2} \rightarrow I_f\,\tfrac{3}{2}) = 1.52 \times 10^{-3} \left[P_{-}(\tfrac{1}{2}\rightarrow\tfrac{3}{2}) G_{E2}(\tfrac{1}{2}\rightarrow\tfrac{3}{2}) \times \right.$$

$$x \left[(I_i \tfrac{1}{2}\, 2\, 1 \mid I_f \tfrac{3}{2}) + (-1)^{I_f+3/2} b_{E2} (I_i \tfrac{1}{2}\, 2, -2 \mid I_f, -\tfrac{3}{2}) \right] +$$

$$+ C(I_i \tfrac{3}{2} \tfrac{1}{2})\, G_{E2}^{coll} (I_i \tfrac{3}{2}\, 2\, 0 \mid I_f \tfrac{3}{2}) +$$

$$+ C(I_f \tfrac{1}{2} \tfrac{3}{2})\, G_{E2}^{coll} (I_i \tfrac{1}{2}\, 2\, 0 \mid I_f \tfrac{1}{2}) \Big]^2 \qquad (15)$$

where higher order terms in the amplitude C have been neglected. When the model values of G_{E2}, b_{E2} and the Coriolis matrix element $\langle \frac{1}{2} \mid j_- \mid \frac{3}{2} \rangle$ together with $P_- (\frac{1}{2} \rightarrow \frac{3}{2}) = 1$ are inserted into eq. (15), we find that the first term is larger than the sum of the two others for all the transitions involved and for reasonable deformation parameters. As, however, the K = 1/2 and K = 3/2 orbitals are located roughly equidistant on each side of the Fermi surface, we expect*) that $\mid P_- (\frac{1}{2} \rightarrow \frac{3}{2}) \mid$ to be of the order of 0.1 or less. This means that the influence of the first term is strongly reduced and that the Coriolis coupling terms become relatively important. The magnitude of these latter terms is directly proportional to the Coriolis coupling matrix element $\langle \frac{1}{2} \mid j_- \mid \frac{3}{2} \rangle$ which, unfortunately, according to the model predictions passes through zero at the relevant deformation $\delta \approx 0.2$, tending to make the predicted values unreliable. In table 3 we give the predicted value of B(E2) for the two values of $P_- (\frac{1}{2} \rightarrow \frac{3}{2}) = 1$ and 0.1 together with the experimental findings. Albridge et al. [1] are the only group to have reported a definite E2 admixture in the transitions between the K = 1/2 and 3/2 bands, while the other groups [2, 3] only give upper limits. The experimental results are not consistent with each other (see table 3), the electron data of Albridge et al. giving consistently higher B(E2)-values. To obtain agreement with Albridge et al. we would have to increase the absolute value of the Coriolis coupling matrix element $\langle \frac{1}{2} \mid j_- \mid \frac{3}{2} \rangle$ by up to 3 units (theory gives $\langle \frac{1}{2} \mid j_- \mid \frac{3}{2} \rangle = -0.3$ for

*) As the experimental data with which to compare the calculated B(E2)-values are very scarece in this case, we have not found it worth while to make a full BCS calculation of the pairing factor $P_- (\frac{1}{2} \rightarrow \frac{3}{2})$.

$\delta = 0.3$). An increased value of $\langle \frac{1}{2} | j_- | \frac{3}{2} \rangle$ is also required for explaining the M1 transition rates between the same bands (see sub-section 4.5).

4.3 E2 transitions with $|\Delta K| = 2$

Only one E2, $|\Delta K| = 2$ transition probability (proceeding between the 1/2 1/2→ 5/2 5/2 levels) has been determined in this work. This transition is found to have nearly single particle strength (see table 1). For the two E2 transitions from the 3/2 1/2 level to the members of the 5/2 ground state band only upper limits of B(E2) can be set (see table 1). There is a drastic difference between the observed E2, $|\Delta K| = 2$ transition rate and the strongly enhanced E2, $|\Delta K| = 1$ transition rates (see above). This is interpreted as being due to the fact that in the $|\Delta K| = 2$ case no Coriolis coupling can mix the initial and final states directly with each other and thereby cause large collective E2 contributions to occur in the transition rates. In principle, second-order Coriolis coupling can take place between the K = 1/2 and K = 5/2 bands via the K = 3/2 band, but in this case only contributions with single-particle strengths would then be obtained. It has also been argued [21] whether or not a direct $|\Delta K| = 2$ coupling of appreciable strength can occur. Fig. 2 shows a compilation of hindrance factors F_N for E2, $|\Delta K| = 2$ transitions as a function of the energy difference between the two states with the same angular momentum which will mix the two pertinent rotational bands (e.g. the energy difference between the 5/2 1/2→ 5/2 5/2 levels in the ^{233}U case). There seems to be a general trend that the enhancement of the E2, $|\Delta K| = 2$ transition rates are increased as the energy difference between admixed states is lowered. This indicates the presence of some kind of mixing between the members of the bands with $|\Delta K| = 2$, either of the direct $|\Delta K| = 2$, of of the second-order Coriolis type. In ^{233}U, where the 5/2 1/2 → 5/2 5/2 energy difference is $\sim$ 460 keV, the effect from such $|\Delta K| = 2$ mixing is expected to be small (see fig. 2). It should also be pointed out that mixing with the γ-vibrational band built on the ground state may be of importance, especially when the

distance between the mixing states is roughly equal to the phonon energy.

In the present case the reduced E2, $|\Delta K| = 2$ transition probability can be written

$$B(E2,\ I_i \tfrac{1}{2} \rightarrow I_f \tfrac{5}{2}) = 1.53 \times 10^{-3} \times$$

$$\times \left[P_- (\tfrac{1}{2} - \tfrac{5}{2})\, G_{E2}(\tfrac{1}{2} \rightarrow \tfrac{5}{2})\, \langle I_i \tfrac{1}{2}\, 2\, 2 \,|\, I_f \tfrac{5}{2} \rangle \right]^2 \qquad (16)$$

the admixtures from the K = 3/2 band giving less than 2 % contribution to the E2 transition rate.

The influence from admixtures of the gamma-vibrational bands is also expected to be small as the vibrational transition strength in this mass region is only 1-3 single particle units [25].

The experimental value of $B(E2,\ \frac{1}{2}\frac{1}{2} \rightarrow \frac{5}{2}\frac{5}{2}) = (8 \pm 4)\ 10^{-3}\ e^2b^2$ has been used to evaluate $P_- G_{E2}$ in eq. (16). We obtain

$$P_-(\tfrac{1}{2} \rightarrow \tfrac{5}{2})\, G_{E2}\, (\tfrac{1}{2} \rightarrow \tfrac{5}{2}) = \pm\, (2.3 \pm 0.6) \qquad (17)$$

This value was then used to calculate the reduced E2, $|\Delta K| = 2$ transition probabilities from the 3/2 1/2 level as $B(E2,\ \frac{3}{2}\frac{1}{2} \rightarrow \frac{5}{2}\frac{5}{2}) = (4.7 \pm 2.4)\ 10^{-3}$ and $B(E2,\ \frac{3}{2}\frac{1}{2} \rightarrow \frac{7}{2}\frac{5}{2}) = (3.5 \pm 1.8)\ 10^{-3}$. These values are then to be compared with the lower limits of B(E2) given from the experiment (table 1). Agreement within two times the statistical errors is obtained.

The result in eq. (17) can now be compared with theoretical expectations for the $P_-(\frac{1}{2} \rightarrow \frac{5}{2})$ and $G_{E2}(\frac{1}{2} \rightarrow \frac{5}{2})$ quantities. As the K = 1/2 to K = 5/2 transitions go from a $\sim$ 400 keV excited orbital to the ground state (Fermi level), we expect $P_-(\frac{1}{2} \rightarrow \frac{5}{2}) = 0.7 \pm 0.3$. This means that $G_{E2}(\frac{1}{2} \rightarrow \frac{5}{2}) = \pm\, (3.3 \pm 1.6)$ which should be compared with the theoretical estimates $G_{E2}(\frac{1}{2} \rightarrow \frac{5}{2}) = -1.86$ ($\delta = 0.2$) and -2.00 ($\delta = 0.3$). Agreement within overlapping errors is obtained.

4.4 M1 transition rates within bands

The M1 transition rates within a rotational band with $K \neq 1/2$ are expected to be described by only one parameter, $(g_K - g_R)$. In the case of a $K = 1/2$ band, one additional parameter b_o has to be included to take the decoupling effect into account. The following expression is valid [17]

$$B(M1,\ I_i K \rightarrow I_f K) = \frac{3}{4\pi} \left(\frac{e\hbar}{2Mc}\right)^2 \langle I_i K 1 0 \mid I_f K \rangle^2$$

$$K^2 (g_K - g_R)^2 \left[1 + \delta_{K,\,1/2} b_o (-1)^{I_> + 1/2}\right]^2 \qquad (18)$$

where $I_>$ denotes the larger of I_i and I_f. From experimental values of, for instance, B(M1) the parameters $(g_K - g_R)$ and b_o can be evaluated and the result be compared with theoretical predictions.

The K = 5/2 band. We have not measured any B(M1)-value in this band. A deduction of the g_K and g_R parameters for this band is given in ref. [19].

The K = 3/2 band. The B(M1) strength of the 28.5 keV transition has been deducd from the half life of the 340.5 keV level and electron intensity data given in table 1 as

$$B(M1,\ 5/2\ 3/2 \rightarrow 3/2\ 3/2) = (4.8 \pm 1.5) 10^{-2} \left(\frac{e\hbar}{2Mc}\right)^2 \qquad (19)$$

Using eqs. (18) and (19) we obtain $g_K - g_R = \pm (0.58 \pm 0.09)$. According to the Nilsson model [5] the parameter g_K can be evaluated from

$$g_K = g_\ell + \frac{[g_s(\mathrm{eff}) - g_\ell]}{2K} \sum (a^2_{\ell,\,K-1/2} - a^2_{\ell,\,K+1/2}) \qquad (20)$$

where for a neutron transition $g_\ell = 0$ and $g_s(\mathrm{eff}) = p\, g_s(\mathrm{free})$ with $g_s(\mathrm{free}) = -3.826$. The amplitudes $a_{\ell,\Omega}$ ($\Omega = K \pm 1/2$) have been

tabulated by Nilsson [5]. In fig. 3 $(g_K - g_R)$ has been plotted as a function of the deformation parameter δ for different values of p. In this diagram the experimental value eq. (19) is also shown. Experiment gives a slightly higher absolute value of $g_K - g_R$ than predicted from the model using $g_R = 0.3$. Such a deviation should, however, not be taken too seriously, as we have not investigated the influence on the predicted values for small variations in the potential parameters $\varkappa$ und μ. We also observe that better agreement is obtained for a larger value of the deformation parameter δ than 0.16 ± 0.03 obtained in subsection 4.1. We have noticed that Coriolis admixtures will only change the predicted values of g_K by roughly 5 per cent.

4.5 M1 transitions with $|\Delta K| = 1$

In the case of M1 transitions we have no dominating collective contributions to the transition probability. Although the Coriolis mixing is therefore not expected to have any decisive influence on the K-allowed M1 transition rates, it may yet influence the detailed structure of the M1 transition rates. Furthermore the pairing correlations are as a rule expected to be of little importance in this case as the paring factors P_+ are generally close to one. In the case, however, when the intrinsic excitations involve single particle states on each side of the Fermi surface, the paring factors may be well below one. The main variations of the predicted B(M1)-values is caused through the uncertainties in the parameter values of $g_s(\text{eff})$, g_R and δ (see below).

$K = 3/2 \rightarrow K = 5/2$ M1 transitions. The reduced M1 transition probability can in this case be written

$$B(M1,\ I_i \tfrac{3}{2} \rightarrow I_f \tfrac{5}{2}) = 5.91 \times 10^{-2} \Big[P_+(\tfrac{3}{2} \rightarrow \tfrac{5}{2}) G_{M1}(\tfrac{3}{2} \rightarrow \tfrac{5}{2}) \times$$

$$\times (I_i \tfrac{3}{2}\ 11 \mid I_f \tfrac{5}{2}) + C(I_f \tfrac{3}{2} \tfrac{5}{2}) G_{M1}(\tfrac{3}{2} \rightarrow \tfrac{3}{2}) (I_i \tfrac{3}{2}\ 10 \mid I_f \tfrac{3}{2}) +$$

$$+ C(I_i \tfrac{5}{2} \tfrac{3}{2}) G_{M1}(\tfrac{5}{2} \rightarrow \tfrac{5}{2})(I_i \tfrac{5}{2} 10 \,|\, I_f \tfrac{5}{2})\Big]^2 \qquad (21)$$

where higher order terms in the amplitude C have been neglected. Using the predicted values for all quantities in eq. (21) we find that the first term is roughly one order of magnitude larger than the sum of the other two. We also notice that both $G_{M1}(\frac{3}{2} \rightarrow \frac{5}{2})$ and the Coriolis matrix element $\langle \frac{3}{2} | j_- | \frac{5}{2} \rangle$ included in the amplitudes C [see eq. (13)] are asymptotically forbidden. We therefore determine $P_+(\frac{3}{2} \rightarrow \frac{5}{2}) G_{M1}(\frac{3}{2} \rightarrow \frac{5}{2})$ and $\langle \frac{3}{2} | j_- | \frac{5}{2} \rangle$ from a least squares fit using eq. (21) supplied with our three different experimental $B(M1, I_i \frac{3}{2} \rightarrow I_f \frac{5}{2})$-values. This fit was performed for several sets of the parameters $g_s(\text{eff})$ [= 80, 60 and 40 % of $g_s(\text{free})$], g_R (= = 0.3 and 0.4) and δ (= 0.2 and 0.3), used in the evaluation of the diagonal quantities $G_{M1}(\frac{3}{2} \rightarrow \frac{3}{2})$ and $G_{M1}(\frac{5}{2} \rightarrow \frac{5}{2})$. We find that the quantity $P_+(\frac{3}{2} \rightarrow \frac{5}{2}) G_{M1}(\frac{3}{2} \rightarrow \frac{5}{2})$ is almost independent of the choice of parameters and consistently comes out as $\pm$ (0.34 $\pm$ 0.08). We expect that $0.9 < P_+(\frac{3}{2} \rightarrow \frac{5}{2}) < 1.0$ to hold implying $G_{M1}(\frac{3}{2} \rightarrow \frac{5}{2})$ = = $\pm$ (0.36 $\pm$ 0.10). In fig. 4 this experimental value is compared with model predictions. We see that good agreement is obtained for the reasonable choice of parameters $g_s(\text{eff}) = (0.6 \pm 0.1) g_s(\text{free})$, $g_R = (0.35 \pm 0.5)$ and $\delta = 0.25 \pm 0.05$.

The Coriolis matrix element $\langle \frac{3}{2} | j_- | \frac{5}{2} \rangle$, which only enters in correction terms in eq. (21), is found in most cases to have an absolute value between 0.3 and 1.0. The sign is in all cases the same as for $G_{M1}(\frac{3}{2} \rightarrow \frac{5}{2})$, in disagreement to the model calculation. Although this determination of $\langle \frac{3}{2} | j_- | \frac{5}{2} \rangle$ is not very accurate there is a tendency for this Coriolis matrix element to be slightly lower than predicted. This is in agreement with the findings in sub-section 4.2 where a more accurate determination of $\langle \frac{3}{2} | j_- | \frac{5}{2} \rangle$ is made from the E2, $|\Delta K| = 1$ transition probability data.

<u>K = 1/2 → K = 3/2 M1 transitions.</u> In this case the only absolute reduced M1 transition probability which has been deduced is $B(M1, \frac{1}{2} \frac{1}{2} \rightarrow \frac{3}{2} \frac{3}{2}) = (10 \pm 5) 10^{-2} \times (\frac{e\hbar}{2Mc})^2$. From the measured relative gamma ray intensities of the two transitions de-exciting

the $3/2\ 1/2^+(631)$ level we also find $B(M1, \frac{3}{2}\frac{1}{2} \rightarrow \frac{5}{2}\frac{3}{2}) / B(M1, \frac{3}{2}\frac{1}{2} \rightarrow \frac{3}{2}\frac{3}{2}) = 3.2 \pm 0.2$. According to the pure Nilsson model this ratio should be independent of the parameters g_s, g_R and δ and only be given by a ratio between two Clebsch-Gordan coefficients, giving the value 1.5. This definite disagreement with the model predictions indicates that Coriolis coupling contributions are of importance. The reduced M1 transition probability can in this case be written

$$B(M1, I_i \tfrac{1}{2} \rightarrow I_f \tfrac{3}{2}) = 5.91 \times 10^{-2} \Big[P_+(\tfrac{1}{2} \rightarrow \tfrac{3}{2}) G_{M1}(\tfrac{1}{2} \rightarrow \tfrac{3}{2}) \times$$

$$(I_i \tfrac{1}{2}\ 11 \mid I_f \tfrac{3}{2}) + C(I_i \tfrac{3}{2}\tfrac{1}{2}) G_{M1}(\tfrac{3}{2} \rightarrow \tfrac{3}{2})(I_i \tfrac{3}{2}\ 10 \mid I_f \tfrac{3}{2}) +$$

$$+ C(I_f \tfrac{1}{2}\tfrac{3}{2}) G_{M1}(\tfrac{1}{2} \rightarrow \tfrac{1}{2}) \quad \big[(I_i \tfrac{1}{2}\ 10 \mid I_f \tfrac{1}{2}) +$$

$$+ b_{M1}(-1)^{I_f + 1/2} (I_i \tfrac{1}{2}\ 1, -1 \mid I_f, -\tfrac{1}{2}) \big] \Big]^2 \qquad (22)$$

where higher order terms in the amplitude C have been neglected. The first term should again be the dominating one but, as pointed out above, Coriolis coupling is for experimental reasons expected to be of importance. Although the quantities $G_{M1}(\frac{1}{2} \rightarrow \frac{3}{2})$ and $\langle \frac{1}{2} \mid j_- \mid \frac{3}{2} \rangle$ are asymptotically allowed, the detailed theoretical estimates of B(M1) can be uncertain since the predicted Coriolis matrix element passes through zero for a deformation close to $\delta = 0.2$. We therefore prefer to deduce $P_+(\frac{1}{2} \rightarrow \frac{3}{2}) G_{M1}(\frac{1}{2} \rightarrow \frac{3}{2})$ and $\langle \frac{1}{2} \mid j_- \mid \frac{3}{2} \rangle$ from eq. (22) using the experimental information mentioned above. The quantities $G_{M1}(\frac{1}{2} \rightarrow \frac{1}{2})$, b_{M1} and G_{M1} are taken as equal to the Nilsson predictions. The values of $P_+(\frac{1}{2} \rightarrow \frac{3}{2}) G_{M1}(\frac{1}{2} \rightarrow \frac{3}{2})$ and $\langle \frac{1}{2} \mid j_- \mid \frac{3}{2} \rangle$ were deduced for several sets of the parameters g_s(eff), g_R and δ. It then turned out that $P_+(\frac{1}{2} \rightarrow \frac{3}{2}) G_{M1}(\frac{1}{2} \rightarrow \frac{3}{2})$ was rather insensitive to the values of these parameters and we consistently found that $P_+(\frac{1}{2} \rightarrow \frac{3}{2}) G_{M1}(\frac{1}{2} \rightarrow \frac{3}{2}) = (1.3 \pm 0.1)$. As the $K = 1/2$ and $K = 3/2$ orbitals are situated on each side of the Fermi surface, the pure independent particle model gives $P_+(\frac{1}{2} \rightarrow \frac{3}{2}) = 0$. Due to the diffuseness of the Fermi surface caused by the pairing correlations $P_+(\frac{1}{2} \rightarrow \frac{3}{2})$ will approach 1.

For a choice of parameters $g_s(\text{eff}) = 0.5\, g_s(\text{free})$, $g_R = 0.3 \pm 0.1$ and $\delta = 0.2$, theory predicts $G_{M1}(\frac{1}{2} \rightarrow \frac{3}{2}) = -1.3$. The value found for $\langle \frac{1}{2} | j_- | \frac{3}{2} \rangle$ was more dependent on the choice of parameters, especially on δ and $g_s(\text{eff})$. To obtain agreement with experiment, using reasonable values for the parameters, we had to choose $\langle \frac{1}{2}^+(631) | j_- | \frac{3}{2}^+(631) \rangle = \pm (1.0 \pm 0.4)$. This means that a much stronger Coriolis coupling between the $K = 1/2$ and $K = 3/2$ bands, than predicted by the Nilsson model $\left[\langle \frac{1}{2} | j_- | \frac{3}{2} \rangle = 0.053\ (\delta = 0.2)$ and $-0.30\ (\delta = 0.3)\right]$, is necessary to explain the observed M1 transition rates. As was pointed out in sub-section 4.2 this large Coriolis coupling is also needed in order to understand the observed enhancements of the E2 transition rates between the $K = 1/2$ and $K = 3/2$ bands.

4.6 The M1, $|\Delta K| = 2$ transition

The only transition in ^{233}U belonging to this group is the 415.8 keV M1 transition between the 3/2, 1/2 → 5/2, 5/2 levels. The M1 part of this transition is strictly forbidden according to the Nilsson model, while the E2 part is allowed. This feature is reflected in the observed high E2 content (> 70 % E2) in the 415.8 keV transition. That the M1 transition exists at all, is usually understood in terms of Coriolis admixtures of bands having a K quantum number intermediate those of the initial and final bands. In the present case the M1 transition can take place via admixtures from the $K = 3/2$ band. The reduced M1 transition probability can be written

$$B(M1, \tfrac{3}{2}\tfrac{1}{2} \rightarrow \tfrac{5}{2}\tfrac{5}{2}) = 5.91 \times 10^{-2} \Big[C(\tfrac{5}{2}\tfrac{3}{2}\tfrac{5}{2}) P_+(\tfrac{1}{2} \rightarrow \tfrac{3}{2}) G_{M1}(\tfrac{1}{2} \rightarrow \tfrac{3}{2}) \times$$

$$\langle \tfrac{3}{2}\tfrac{1}{2}\, 11 \,|\, \tfrac{5}{2}\tfrac{3}{2} \rangle + C(\tfrac{3}{2}\tfrac{3}{2}\tfrac{1}{2}) P_+(\tfrac{3}{2} \rightarrow \tfrac{5}{2}) G_{M1}(\tfrac{3}{2} \rightarrow \tfrac{5}{2}) \times$$

$$\langle \tfrac{3}{2}\tfrac{3}{2}\, 11 \,|\, \tfrac{5}{2}\tfrac{5}{2} \rangle \Big]^2 \qquad (23)$$

where we have neglected terms to higher order in the amplitude C.

All the pertinent matrix elements in eq. (23) have been experimentally determined in the previous sub-sections and in some cases been found to deviate from theoretical predictions. We have therefore calculated $B(M1, \frac{3}{2}\frac{1}{2} \rightarrow \frac{5}{2}\frac{5}{2})$ using only such matrix elements which have earlier been found to be in accordance with our experimental data (sub-sections 4.1 - 4.5). The following quantities have been used: $P_+(\frac{1}{2} \rightarrow \frac{3}{2}) G_{M1}(\frac{1}{2} \rightarrow \frac{3}{2}) = -1.3$ (in accordance with the model), $\langle \frac{3}{2} | j_- | \frac{5}{2} \rangle = +0.35$ (the model predicts $+1.2 \pm 0.1$), $G_{M1}(\frac{3}{2} \rightarrow \frac{5}{2}) = -0.36$ (in accordance with the model) and $\langle \frac{1}{2} | j_- | \frac{3}{2} \rangle = -2.0$ (the model predicts -0.1 ± 0.2). When these values are put into eq. (23) we find that the second term is roughly a factor of five larger than the first term, and we get $B(M1, \frac{3}{2}\frac{1}{2} \rightarrow \frac{5}{2}\frac{5}{2}) = 4 \times 10^{-4} (\frac{e\hbar}{2Mc})^2$ which is in agreement with our experimental value of $> 2 \times 10^{-4} (\frac{e\hbar}{2Mc})^2$. This shows that the matrix elements deduced from our experimental data from a consistent set which, put into eq. (23), is enough to explain the occurrence of the (3/2, 1/2 → 5/2, 5/2), M1, K-forbidden transition through Coriolis mixing.

5. SUMMARY AND CONCLUSIONS

The 22 reduced B(M1) and B(E2) transition probabilities (including 9 limits) deduced from the half life measurements in the present investigation, together with earlier electron intensity data [1, 2, 3] can be divided into 6 groups. From the transition rates within bands (sub-sections 4.1 and 4.4) we obtain information on the quantities δ and $(g_K - g_R)$.

From the E2, $|\Delta K| = 1$ transitions between the K = 3/2 and K = 5/2 bands we obtain an indication that the asymptotically forbidden Coriolis matrix element $\langle \frac{3}{2}^+(631) | j_- | \frac{5}{2}^+(633) \rangle$ might be overestimated by roughly a factor of three by the Nilsson model. This is in accordance with the weaker evidences from the corresponding M1, $|\Delta K| = 1$ transition rates.

In the case of the K = 1/2 and K = 3/2 bands, the model predicts weak Coriolis mixing. In fact $\langle \frac{1}{2} | j_- | \frac{3}{2} \rangle$ is predicted to be practically zero at a deformation of $\delta \approx 0.2$. From our experimental data, the evidence from the pertinent E2, $|\Delta K| = 1$, M1, $|\Delta K| = 1$ and M1, $|\Delta K| = 2$ transition rates seem to indicate much larger Coriolis mixing between the K = 1/2 and K = 3/2 bands.

We thus find that both the asymptotically forbidden $\langle \frac{3}{2}^+(631) \mid j_- \mid \frac{5}{2}^+(633) \rangle$, and the asymptotically allowed $\langle \frac{1}{2}^+(631) \mid j_- \mid \frac{3}{2}^+(631) \rangle$ Coriolis matrix elements do not seem to be well accounted for by the model, at least using the potential parameters $\varkappa = 0.05$ and $\mu = 0.45$ for $N = 5$.

On the other hand we find that both $G_{M1}(\frac{1}{2} \rightarrow \frac{3}{2})$ and $G_{M1}(\frac{3}{2} \rightarrow \frac{5}{2})$ seem to be reasonably well accounted for using the same potential parameters and in addition an effective gyromagnetic factor, g_s, equal to (0.6 ± 0.1) times the free nucleon value.

ACKNOWLEDGEMENT

We are very indepted to Dr. Sven Wahlborn for his critical examination of the manuscript.

REFERENCES

1. ALBRIDGE R G, HOLLANDER J M, GALLAGHER C J and HAMILTON J H,
The energy levels of U^{233}.
Nuclear Physics 27 (1961) 529 (UCRL-9438-Rev.).

2. SCHULTZE G and AHLF J,
Excited states of Uranium-233.
Nuclear Physics 30 (1962) 163 (in German).

3. BISGÅRD K M, DAHL P, HORNSHØJ P and KNUTSEN A B,
The beta decay of Pa^{233}.
Nuclear Physics 41 (1963) 21.

4. ROSE M E,
Internal conversion coefficients.
North-Holland Publ. Co., Amsterdam, 1958.

5. NILSSON S G,
Binding states of individual nucleons in strongly deformed nuclei.
Mat. Fys. Medd. Dan. Vid. Selsk. 29 (1955) No. 16.

6. WAHLBORN S,
Variational approach to the nuclear pairing-correlation problem.
Arkiv Fysik 31 (1965) 33.
The nuclear pairing-correlation model. 2.
Arkiv Fysik 31 (1966) 319.

7. KERMAN A K,
Rotational perturbations in nuclei-application to W^{183}.
Mat. Fys. Medd. Dan. Vid. Selsk. 30 (1956) No. 15.

8. BROCKMEIER R T, WAHLBORN S, SEPPI E J and BOEHM F,
Coriolis coupling between rotational bands in the nucleus W^{183}.
Nuclear Physics 63 (1965) 102.

9. GERHOLM T R and LINDSKOG J,
A magnetic coincidence spectrometer for the measurement of short nuclear lifetimes.
Arkiv Fysik 24 (1963) 171.

10. SPARRMAN P, LINDSKOG J and MARELIUS A,
An electron scintillation detector with good energy resolution.
Nuclear Instr. and Methods 41 (1966) 299.

11. GRAHAM R L, GEIGER J S, BELL R E and BARTON R,
A simple and accurate method for calibrating nanosecond time-to-pulse-height converters.
Nuclear Instr. and Methods 15 (1962) 40.

12. MALMSKOG S G,
Absolute E1 transition probabilities in the deformed nuclei Yb^{177} and Hf^{179}.
Nuclear Physics 62 (1965) 37.

13. LINDSKOG J and SUNDSTRÖM T,
Improved experimental methods for measurements of nuclear lifetimes down to 10^{-11} seconds.
Arkiv Fysik 24 (1963) 199.

14. WAPSTRA A H, NIJGH G J and van LIESHOUT R,
Nuclear Spectroscopy Tables.
North-Holland Publ. Co., Amsterdam, 1959.

15. JOHANSSON B and ALVÄGER T,
The high-frequency deflection method for measuring short half-lives. Part. 1.
Arkiv Fysik 17 (1960) 163.

16. BELL R E, BJØRNHOLM S and SEVERIENS J C,
Half lives of first excited states of even nuclei of Em, Ra, Th, U, and Pu.
Mat. Fys. Medd. Dan. Vid. Selsk. 32 (1960) No. 12.

17. NATHAN O and NILSSON S G,
in Alpha-, beta- and gamma-ray spectroscopy.
Ed. K. Siegbahn. North-Holland Publ. Co., Amsterdam, 1965. Chap. 10.

18. DORAIN P B, HUTCHISON C A, Jr. and WONG E,
Paramagnetic resonance absorption in uranium (III) chloride in the nuclear spin, magnetic dipole moment, and electric quadrupole moment of uranium-233.
Phys. Rev. 105 (1957) 1307.

19. NEWTON J O,
The Coulomb excitation of U^{233} and Np^{237} and a discussion of the energy levels of U^{233}.
Nuclear Physics 5 (1958) 218.

20. CHU Y Y and PERLMAN M L,
Empirical screening correction for M-subshell internal conversion coefficients.
Phys. Rev. 135 (1964) B 319.

21. LÖBNER K E G and MALMSKOG S G,
Systematics of absolute gamma-ray transition probabilities in deformed odd-mass nuclei.
Nuclear Physics 80 (1966) 505.

22. FAESSLER A,
The influence of the pairing correlations and the Coriolis force on the E2 $|\Delta K| = 1$ transitions in deformed odd-mass nuclei.
Nuclear Physics 85 (1966) 679.

23. SOBICZEWSKI A,
Equilibrium deformations of heavy nuclei calculated with projected wave functions.
Nuclear Physics A96 (1967) 258.

24. MALMSKOG S G and WAHLBORN S,
(To be published in Nuclear Physics.)

25. ELBEK B,
Determination of nuclear transition probabilities by Coulomb excitation.
Copenhagen 1963, Thesis.

Table 1

Level in keV	$T_{\frac{1}{2}}$ (exp) of level in psec.	Transition in keV	Initial state $IK^{\pi}[Nn_z\Lambda]$	Final state $IK^{\pi}[Nn_z\Lambda]$	Multipolarity	Relative N_γ a)	Relative N_e a)	$T_{\frac{1}{2}\gamma}$ (exp) in sec.	B(M1)↓ in $\left(\frac{e\hbar}{2Mc}\right)^2$	B(E2)↓ in e^2b^2	Errors in %	Average B(M1) and B(E2) values	F_W	F_N c)
311.9	120±15	311.9	3/2 3/2+(631)	5/2 5/2+(633)	M1	34	34	2.4(-10)	5.4(-3)	—	25		320	15.5
						34	34	2.4(-10)	5.4(-3)	—	25	$(5.4\pm1.4)\times10^{-3}$	320	15.5
						34	34	2.4(-10)	5.4(-3)	—	25		320	15.5
					E2	<0.7	—	>1.2(-8)	—	<2.0(-3)			>5.2	>1.2(-2)
						<1.0	—	>8.1(-9)	—	<2.8(-3)	b)	$<2.0\times10^{-3}$	>3.7	>8.0(-2)
						—	—	—	—	—			—	—
		271.6		7/2 5/2+(633)	E2	0.39	0.11	2.1(-8)	—	1.8(-3)	40		4.7	1.4(-2)
						0.45	0.12	1.9(-8)	—	2.1(-3)	40	$(1.8\pm0.8)\times10^{-3}$	4.3	1.3(-2)
						0.34	0.09	2.4(-8)	—	1.6(-3)	40		5.4	1.6(-2)
340.5	52±10	340.5	5/2 3/2+(631)	5/2 5/2+(633)	M1	4.0	2.9	5.0(-10)	2.0(-3)	—	35		880	12
						4.14	3.2	4.5(-10)	2.2(-3)	—	30	$(2.0\pm0.6)\times10^{-3}$	790	11
						3.8	3.0	5.2(-10)	1 9(-3)	—	25		910	13
					E2	<0.8	—	>2.5(-9)	—	<4.9(-3)	—		>1.7	4.0(-3)
						0.36	—	5.2(-9)	—	2.4(-3)	75	$(2.4\pm1.8)\times10^{-3}$	3.6	8.0(-3)
						—	—	—	—	—	—		—	—
		300.2		7/2 5/2+(633)	M1	5.7	6.5	3.5(-10)	4.2(-3)	—	35		420	14.1
						6.0	6.8	3.1(-10)	4.7(-3)	—	30	$(4.4\pm1.3)\times10^{-3}$	370	12.7
						5.7	6.3	3.5(-10)	4.2(-3)	—	25		420	14.2
					E2	0.78	—	2.5(-9)	—	9.2(-3)	100	$(9.2\pm9.2)\times10^{-3}$	0.93	7.0(-5)
						<0.18	—	>1.0(-8)	—	<2.2(-3)	—	$<2.2\times10^{-3}$	>3.8	>3.0(-4)
						—	—	—	—	—	—	—	—	—
		248.7		9/2 5/2+(633)	E2	0.05	—	4.1(-8)	—	1.5(-3)	40	$(1.5\pm0.6)\times10^{-3}$	5.9	0.017
		28.5		3/2 3/2+(631)	M1	4.6(-2)	19	4.3(-8)	4.0(-2)	—	45		44	
						5.8(-2)	16	3.4(-8)	5.0(-2)	—	30	$(4.8\pm1.5)\times10^{-2}$	35	rot. trans.
						5.7(-2)	20	3.5(-8)	4.9(-2)	—	55		36	
					E2	1.4(-3)	—	1.4(-6)	—	2.1(0)	60		4.0(-3)	
						6.0(-4)	—	3.2(-6)	—	9.4(-1)	40	(1.2±0.4)	9.0(-3)	rot. trans.
						1.1(-3)	—	1.8(-6)	—	1.7(0)	80		5.0(-3)	
398.6	55±20	398.6	1/2 1/2+(631)	5/2 5/2+(633)	E2	1.10	0.10	9.1(-10)	—	6.2(-3)	50		1.4	0.92
						1.37	0.13	7.3(-10)	—	7.7(-3)	50	$(8.0\pm4.0)\times10^{-3}$	1.1	0.79
						1.74	0.16	5.7(-10)	—	9.8(-3)	50		0.9	0.58
		86.6		3/2 3/2+(631)	M1	1.74	15.2	5.7(-10)	0.10	—	50		16	6.8
						1.74	14.3	5.7(-10)	0.10	—	50	$(1.0\pm0.5)\times10^{-1}$	16	6.8
						1.72	14.3	5.8(-10)	0.10	—	50		17	6.9

continuation

Table 1 continuation

Level in keV	$T_{\frac{1}{2}}$ (exp) of level in psec.	Transi-energy in keV	Initial state $IK^{\pi}[Nn_z\Lambda]$	Final state $IK^{\pi}[Nn_z\Lambda]$	Multi-polarity	Relative N_γ a)	Relative N_e a)	$T_{\frac{1}{2}\gamma}$ (exp) in sec.	B(M1)↓ in $(\frac{e\hbar}{2Mc})^2$	B(E2)↓ in e^2b^2	Errors in %	Average B(M1) and B(E2) values	F_W	F_N c)
					E2	3.6 (-2)	—	2.8 (-8)	—	0.41	75		1.9 (-2)	3.6 (-4)
						<3.5 (-3)	—	>2.8 (-7)	—	<4.1 (-2)	b)	$(4.0\pm3.0)\times10^{-1}$	>0.19	>3.6 (-3)
						<3.8 (-2)	—	>2.6 (-8)	—	<4.5 (-1)			>1.7 (-2)	>3.4 (-4)
		57.9		5/2 3/2+(631)	E2	weak	weak	—	—	—	—	—	—	—
415.8	<30	415.8	3/2 1/2+(631)	5/2 5/2+(633)	M1	0.27	0.22	<2.7 (-9)	>2.0 (-4)	—			<8.7 (+3)	IK-forb.
						0.11	0.27	<7.3 (-9)	>7.5 (-5)	—	b)	$>2\times10^{-4}$	<2.4 (+4)	IK-forb.
						0.26	0.21	<2.7 (-9)	>2.0 (-4)	—			<8.7 (+3)	IK-forb.
					E2	1.21	—	<6.0 (-10)	—	>7.6 (-3)	b)		<1.1	<0.43
						2.52	—	<3.1 (-10)	—	>1.5 (-2)		$>6\times10^{-3}$	<0.6	<0.22
						0.93	—	<7.6 (-10)	—	>6.0 (-3)			<1.4	<0.55
		375.4		7/2 5/2+(633)	E2	0.64	0.06	<1.1 (-9)	—	>6.8 (-3)	b)		<1.3	<0.36
						0.56	0.06	<1.2 (-9)	—	>6.2 (-3)		$>6.2\times10^{-3}$	<1.4	<0.40
						0.70	0.09	<1.0 (-9)	—	>7.1 (-3)			<1.1	<0.32
		103.9		3/2 3/2+(633)	M1	0.75	4.02	<9.7 (-10)	>3.6 (-2)	—			<45	<8.1
						0.68	3.42	<1.2 (-9)	>3.0 (-2)	—	b)	$>3.0\times10^{-2}$	<59	<9.8
						0.69	3.42	<1.0 (-9)	>3.5 (-2)	—			<51	<8.5
					E2	3.1 (-2)	—	<2.3 (-8)	—	>0.2			<4.2 (-2)	<1.4 (-5)
						<1.8 (-2)	—	<[>4.4 (-8)]	—	>[<0.11]	b)		<[>8.2 (-2)]	<[>2.7 (-5)]
						<1.4 (-2)	—	<[>5.1 (-8)]	—	>[<9.1(-2)]			<[>9,5 (-2)]	<[>3.2 (-5)]
		75.3		5/2 3/2+(631)	M1	1.05	12.9	<6.9 (-10)	>0.14	—			<13	<3.3
						1.16	13.8	<6.9 (-10)	>0.14	—	b)	$>1.2\times10^{-1}$	<13	<3.3
						0.93	11.1	<7.6 (-10)	>0.12	—			<14	<3.6
					E2	1.1 (-2)	—	<6.6 (-8)	—	>0.35	b)		<2.4 (-2)	<6.0 (-7)
						<6.0 (-4)	—	<[>1.3 (-6)]	—	>[<1.8 (-2)]			<[>0.5]	<[>1.2 (-5)]
						—	—	—	—	—			—	—
		17.3		1/2 1/2+(631)	M1	—	—	—		—			—	
						~1.4 (-3)	4	<5.7 (-7)	>1.3 (-2)	—	b)	$>1.3\times10^{-2}$	<130	rot. trans.
						≲1.8 (-3)	5	≲4.0 (-7)	≳1.9 (-2)	—			≲95	
					E2	—	—	—	—	—			—	
						>1.0 (-4)	—	<8.0 (-6)	—	>4.6	b)	>4.6	<2.0 (-3)	rot. trans.
						—	—	—	—	—			—	

Notations on the next page.

Notations for table 1

(- 3) stands for 10^{-3} and so on. In cases where two limits occur the first one is set from the half life and the other from the E2-admixture.

a) For each transition the normalisation is made such that $Ne/(N_\gamma M1 + N_\gamma E2)$ gives the total conversion coefficient.

b) The errors are included in the limits.

c) The theoretical predictions have been obtained from eqs. using the potential parameters $\varkappa = 0.05$ and $\mu = 0.45$ and a deformation of $\delta = 0.2$. In the case of M1 transitions $g_R = 0.3$ and $g_s = -3.826$ were used.

Table 2

E (keV)	$I_i K_i \rightarrow I_f K_f$	Predicted $B(E2)\downarrow$ $\langle 3/2 \mid j- \mid 5/2\rangle^2 \cdot E^{*2} \cdot Q_o^2$	Measured $B(E2)\downarrow$	$\mid E^* Q_o \langle 3/2 \mid j- \mid 5/2\rangle \mid$ (keV · b)	$\mid \langle 3/2 \mid j- \mid 5/2\rangle \mid$ with $E^* = 5.7$ keV and $Q_o = (10 \pm 3)\, e^2 b^2$
311.9	3/2 3/2 → 5/2 5/2	3.3×10^{-6}	$< 2.0 \times 10^{-3}$	<25	<0.62
271.6	3/2 3/2 → 7/2 5/2	4.4×10^{-6}	$(1.8 \pm 0.8) \times 10^{-3}$	20 ± 5	0.35 ± 0.14
340.5	5/2 3/2 → 5/2 5/2	3.3×10^{-6}	$(2.4 \pm 1.8) \times 10^{-3}$	27 ± 13	0.47 ± 0.27
300.2	5/2 3/2 → 7/2 5/2	1.2×10^{-7}	$(9.2 \pm 9.2) \times 10^{-3}$	$270 \,^{+110}_{-270}$	$4.7 \,^{+2.4}_{-4.7}$
			$< 2 \times 10^{-3}$	<130	<3.3
248.7	5/2 3/2 → 9/2 5/2	7.8×10^{-6}	$(1.5 \pm 0.6) \times 10^{-3}$	14 ± 4	0.25 ± 0.10

Table 3

The $K = 1/2$ to $K = 3/2$ band E2, $|\Delta K| = 1$ transition rates.

Transition	Deformation δ	Predicted E2 transition rates using eq. 15: Mainterm	Sum of diagonal contributions	B(E2)↓-predicted: $P_-(1/2\to 3/2) = 1$	B(E2)↓-predicted: $P_-(1/2\to 3/2) = 0.1$	Experimental values of B(E2)↓
1/2 1/2→3/2 3/2	0.2	$-2.00\, P_-(1/2\to 3/2)$	+ 0.33	4.2×10^{-3}	2.6×10^{-5}	$(4\pm3) \times 10^{-1}$
						$<4.1 \times 10^{-2}$
	0.3	$-2.13\, P_-(1/2\to 3/2)$	- 1.83	2.4×10^{-2}	6.3×10^{-3}	$<4.5 \times 10^{-1}$
3/2 1/2→3/2 3/2	0.2	$-1.43\, P_-(1/2\to 3/2)$	+ 0.09	2.7×10^{-3}	4.3×10^{-6}	>0.2
						>(<0.11)
	0.3	$-1.61\, P_-(1/2\to 3/2)$	- 0.53	7.0×10^{-3}	7.2×10^{-4}	>(<0.09)
3/2 1/2→5/2 3/2	0.2	$1.51\, P_-(1/2\to 3/2)$	+ 0.30	5.0×10^{-3}	3.1×10^{-4}	>0.35
						>(<0.018)
	0.3	$1.63\, P_-(1/2\to 3/2)$	- 1.59	2.4×10^{-6}	3.1×10^{-3}	—

FIGURE CAPTIONS

Fig. 1 On the left-hand side is shown the pertinent part of the electron spectrum from the decay of ^{233}Pa measured with one lens set to 3 % relative momentum resolution. The vertical lines show the different energy settings in the delayed coincidence measurements described in sub-section 2.5. The horisontal arrows ↔ denote the energy setting without high tension, while the arrows ⇔ denote the corresponding energy setting with high tension applied. The right-hand side shows the part of the decay scheme of ^{233}U of interest in this investigation. The width of the vertical arrows is proportional to the total transition intensity, the filled part giving the gamma transition intensity. The intensities of the continuous β branches are obtained from the electron and gamma transition intensity balance. All energies are given in keV.

Fig. 2 The hindrance factors F_N for E2, $|\Delta K| = 2$ transitions are shown as a function of the energy difference between the two states with the same total angular momentum which can mix the two rotational bands with K-quantum numbers K and K + 2. The following symbols are used:

⊠ denotes proton transitions

⊙ denotes neutron transitions

A is transitions from $I_i = K_i$	to $I_f = K_f$
B is transitions from $I_i = K_i$	to $I_f = K_f + 1$
C is transitions from $I_i = K_i$	to $I_f = K_f + 2$
D is transitions from $I_i = K_i + 1$	to $I_f = K_f$
E is transitions from $I_i = K_i + 1$	to $I_f = K_f + 1$

where the subscripts i and f denote the initial and final states of the transition. Transitions between the same states in different nuclei are connected by lines.

Fig. 3 $(g_K - g_R)$ as a function of the deformation parameter δ and the effective gyromagnetic ratio $g_s(\text{eff}) = p \cdot g_s(\text{free})$ for

the $3/2^+(631)$ rotational band in ^{233}U. The theoretical values are calculated from the Nilsson model using the parameter values $\kappa = 0.05$, $\mu = 0.45$ and $g_R = 0.3$.

Fig. 4 The matrix element $G_{M1}(\frac{3}{2} \rightarrow \frac{5}{2})$ (defined in ref. 5) for transitions between the $3/2^+(631)$ and $5/2^+(633)$ Nilsson orbitals calculated for different values of the deformation parameter δ and the collective gyromagnetic ratio g_R. The shaded portion shows the experimental result obtained from at least square fits to our experimental B(M1) data.

Fig. 1

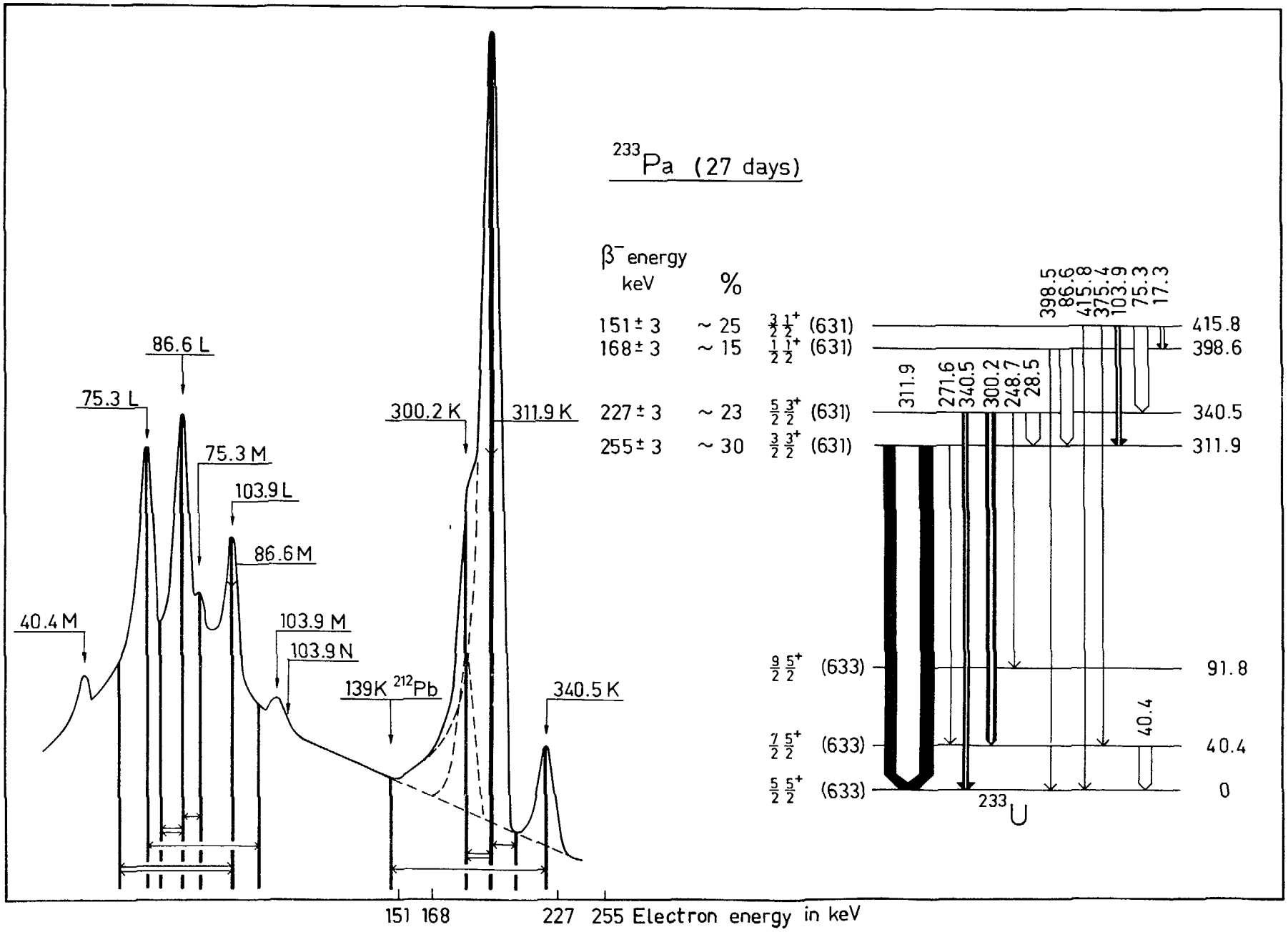
233Pa (27 days)
β⁻ energy
keV
%
151 ± 3 ~ 25
168 ± 3 ~ 15
227 ± 3 ~ 23
255 ± 3 ~ 30
86.6 L
75.3 L
75.3 M
103.9 L
86.6 M
40.4 M
103.9 M
103.9 N
139K 212Pb
300.2 K
311.9 K
340.5 K
151 168 227 255 Electron energy in keV
398.5
86.6
415.8
375.4
103.9
75.3
17.3
311.9
271.6
340.5
300.2
248.7
28.5
40.4
415.8
398.6
340.5
311.9
91.8
40.4
0
(631)
(633)
233U

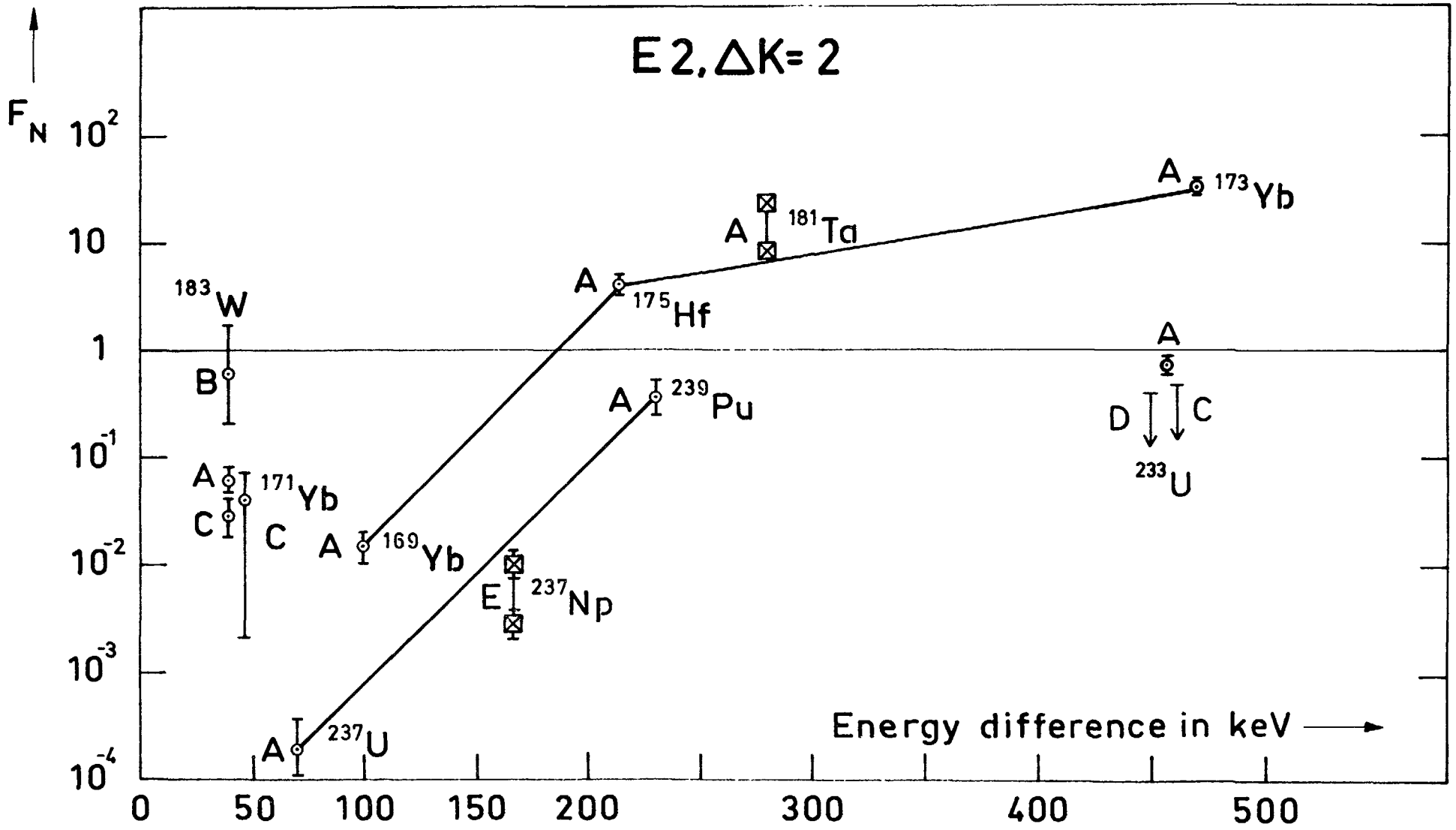
E 2, ΔK= 2
F_N
10^2
10
1
10^-1
10^-2
10^-3
10^-4
183 W
B
A 171 Yb
C
C
A 169 Yb
A 175 Hf
A 181 Ta
A 173 Yb
A 239 Pu
E 237 Np
A 237 U
A
D
C
233 U
Energy difference in keV
0
50
100
150
200
300
400
500

Fig. 2

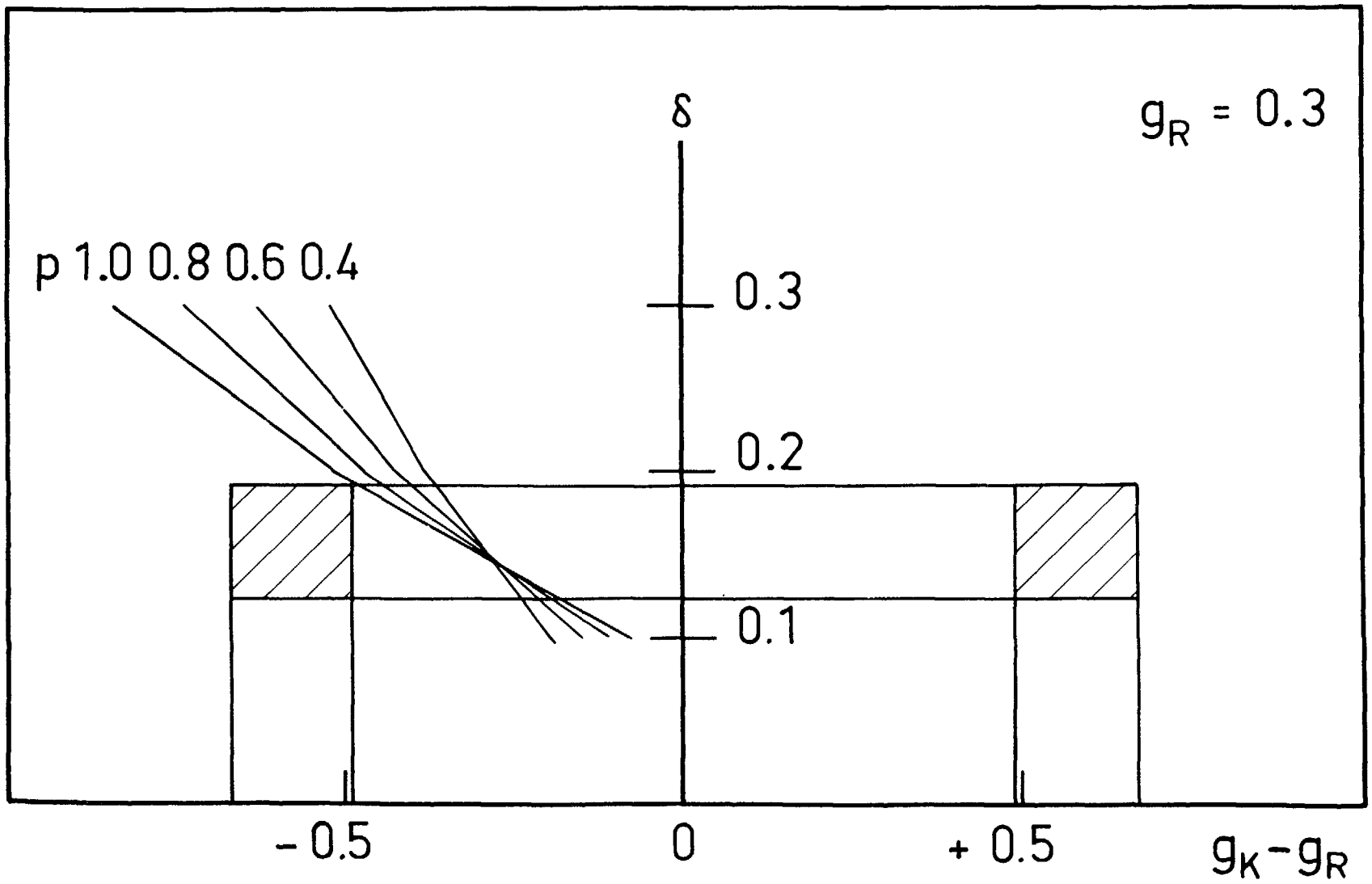

Fig. 3

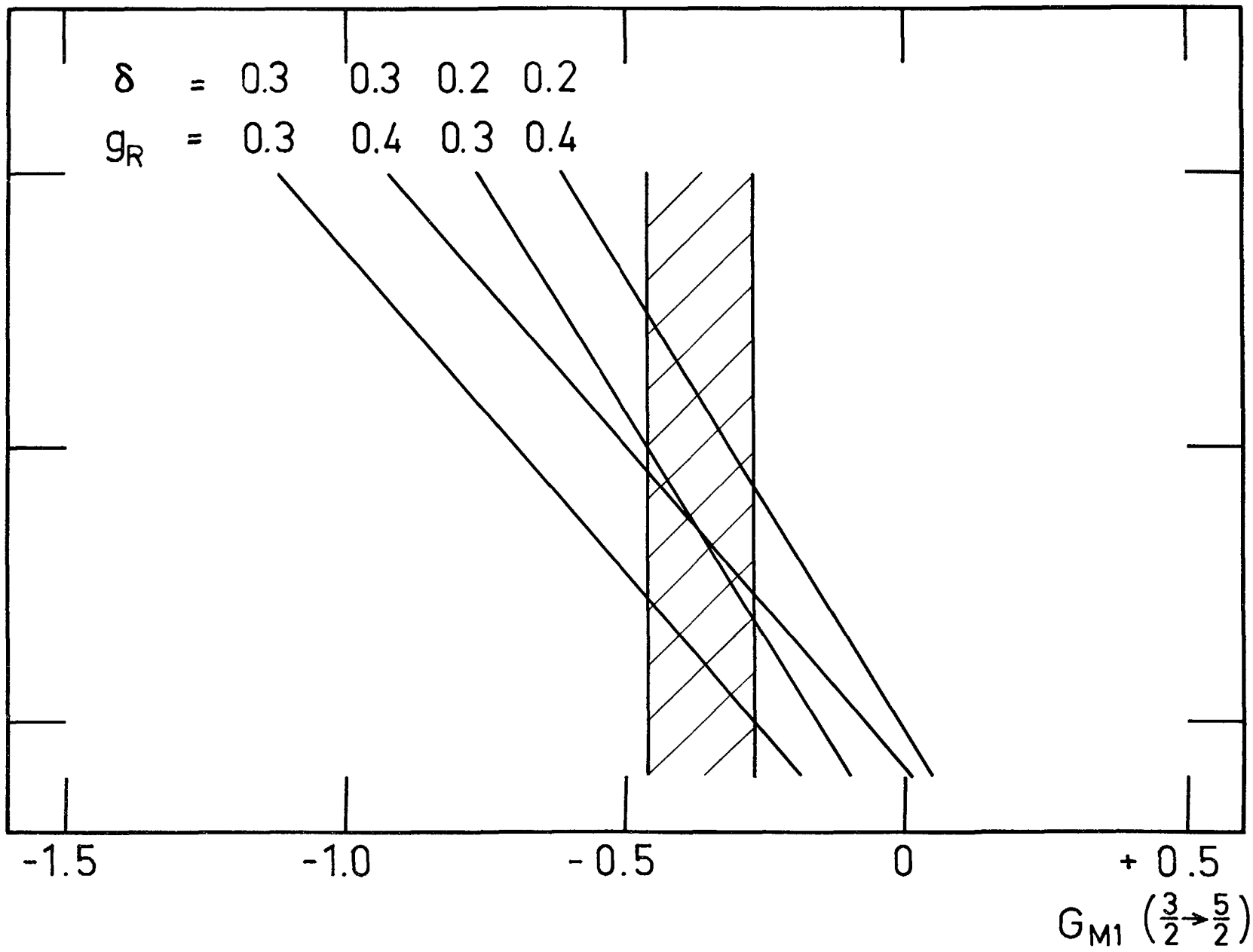
δ = 0.3 0.3 0.2 0.2
g_R = 0.3 0.4 0.3 0.4
-1.5
-1.0
-0.5
0
+0.5
G_{M1} $(\frac{3}{2}\rightarrow\frac{5}{2})$

Fig. 4

LIST OF PUBLISHED AE-REPORTS

1–210. (See the back cover earlier reports.)

211. Report on the personnel dosimetry at AB Atomenergi during 1964. By K. A. Edvardsson. 1966. 15 p. Sw. cr. 8:–.

212. Central reactivity measurements on assemblies 1 and 3 of the fast reactor FR0. By S-O. Londen. 1966. 58 p. Sw. cr. 8:–.

213. Low temperature irradiation applied to neutron activation analysis of mercury in human whole blood. By D. Brune. 1966. 7 p. Sw. cr. 8:–.

214. Characteristics of linear MHD generators with one or a few loads. By E. A. Witalis. 1966. 16 p. Sw. cr. 8:–.

215. An automated anion-exchange method for the selective sorption of five groups of trace elements in neutron-irradiated biological material. By K. Samsahl. 1966. Sw. cr. 8:–.

216. Measurement of the time dependence of neutron slowing-down and thermalization in heavy water. By E. Möller. 1966. 34 p. Sw. cr. 8:–.

217. Electrodeposition of actinide and lanthanide elements. By N-E. Bärring. 1966. 21 p. Sw. cr. 8:–.

218. Measurement of the electrical conductivity of He^3 plasma induced by neutron irradiation. By J. Braun and K. Nygaard. 1966. 37 p. Sw. cr. 8:–.

219. Phytoplankton from Lake Magelungen, Central Sweden 1960–1963. By T. Willén. 1966. 44 p. Sw. cr. 8:–.

220. Measured and predicted neutron flux distributions in a material surrounding av cylindrical duct. By J. Nilsson and R. Sandlin. 1966. 37 p. Sw. cr. 8:–.

221. Swedish work on brittle-fracture problems in nuclear reactor pressure vessels. By M. Grounes. 1966. 34 p. Sw. cr. 8:–.

222. Total cross-sections of U, UO_2 and ThO_2 for thermal and subthermal neutrons. By S. F. Beshai. 1966. 14 p. Sw. cr. 8:–.

223. Neutron scattering in hydrogenous moderators, studied by the time dependent reaction rate method. By L. G. Larsson, E. Möller and S. N. Purohit. 1966. 26 p. Sw. cr. 8:–.

224. Calcium and strontium in Swedish waters and fish, and accumulation of strontium-90. By P-O. Agnedal. 1966. 34 p. Sw. cr. 8:–.

225. The radioactive waste management of Studsvik. By R. Hedlund and A. Lindskog. 1966. 14 p. Sw. cr. 8:–.

226. Theoretical time dependent thermal neutron spectra and reaction rates in H_2O and D_2O. By S. N. Purohit. 1966. 62 p. Sw. cr. 8:–.

227. Integral transport theory in one dimensional geometries. By I. Carlvik. 1966. 65 p. Sw. cr. 8:–.

228. Integral parameters of the generalized frequency spectra of moderators. By S. N. Purohit. 1966. 27 p. Sw. cr. 8:–.

229. Reaction rate distributions and ratios in FRO assemblies 1, 2 and 3. By T. L. Andersson. 1966. 50 p. Sw. cr. 8:–.

230. Different activation techniques for the study of epithermal spectra, applied to heavy water lattices of varying fuel-to-moderator ratio. By E. K. Sokolowski. 1966. 34 p. Sw. cr. 8:–.

231. Calibration of the failed-fuel-element detection systems in the Ågesta reactor. By O. Strindehag. 1966. 52 p. Sw. cr. 8:–.

232. Progress report 1965. Nuclear chemistry. Ed. by G. Carleson. 1966. 26 p. Sw. cr. 8:–.

233. A summary report on assembly 3 of FR0. By T. L. Andersson, B. Brunfelter, P. F. Cecchi, E. Hellstrand, J. Kockum, S-O. Londen and L. I. Tirén. 1966. 34 p. Sw. cr. 8:–.

234. Recipient capacity of Tvären, a Baltic Bay. By P.-O. Agnedal and S. O. W. Bergström. 1966. 21 p. Sw. cr. 8:–.

235. Optimal linear filters for pulse height measurements in the presence of noise. By K. Nygaard. 1966. 16 p. Sw. cr. 8:–.

236. DETEC, a subprogram for simulation of the fast-neutron detection process in a hydro-carbonous plastic scintillator. By B. Gustafsson and O. Aspelund. 1966. 26 p. Sw. cr. 8:–.

237. Microanalys of fluorine contamination and its depth distribution in zircaloy by the use of a charged particle nuclear reaction. By E. Möller and N. Starfelt. 1966. 15 p. Sw. cr. 8:–.

238. Void measurements in the regions of sub-cooled and low-quality boiling. P. 1. By S. Z. Rouhani. 1966. 47 p. Sw. cr. 8:–.

239. Void measurements in the regions of sub-cooled and low-quality boiling. P. 2. By S. Z. Rouhani. 1966. 60 p. Sw. cr. 8:–.

240. Possible odd parity in ^{126}Xe. By L. Broman and S. G. Malmskog. 1966. 10 p. Sw. cr. 8:–.

241. Burn-up determination by high resolution gamma spectrometry: spectra from slightly-irradiated uranium and plutonium between 400–830 keV. By R. S. Forsyth and N. Ronqvist. 1966. 22 p. Sw. cr. 8:–.

242. Half life measurements in ^{155}Gd. By S. G. Malmskog. 1966. 10 p. Sw. cr. 8:–.

243. On shear stress distributions for flow in smooth or partially rough annuli. By B. Kjellström and S. Hedberg. 1966. 66 p. Sw. cr. 8:–.

244. Physics experiments at the Ågesta power station. By G. Apelqvist, P.-Å. Bliselius, P. E. Blomberg, E. Jonsson and F. Åkerhielm. 1966. 30 p. Sw. cr. 8:–.

245. Intercrystalline stress corrosion cracking of inconel 600 inspection tubes in the Ågesta reactor. By B. Grönwall, L. Ljungberg, W. Hübner and W. Stuart. 1966. 26 p. Sw. cr. 8:–.

246. Operating experience at the Ågesta nuclear power station. By S. Sandström. 1966. 113 p. Sw. cr. 8:–.

247. Neutron-activation analysis of biological material with high radiation levels. By K. Samsahl. 1966. 15 p. Sw. cr. 8:–.

248. One-group perturbation theory applied to measurements with void. By R. Persson. 1966. 19 p. Sw. cr. 8:–.

249. Optimal linear filters. 2. Pulse time measurements in the presence of noise. By K. Nygaard. 1966. 9 p. Sw. cr. 8:–.

250. The interaction between control rods as estimated by second-order one-group perturbation theory. By R. Persson. 1966. 42 p. Sw. cr. 8:–.

251. Absolute transition probabilities from the 453.1 keV level in 183W. By S. G. Malmskog. 1966. 12 p. Sw. cr. 8:–.

252. Nomogram for determining shield thickness for point and line sources of gamma rays. By C. Jönemalm and K. Malén. 1966. 33 p. Sw. cr. 8:–.

253. Report on the personnel dosimetry at AB Atomenergi during 1965. By K. A. Edwardsson. 1966. 13 p. Sw. cr. 8:–.

254. Buckling measurements up to 250°C on lattices of Ågesta clusters and on D_2O alone in the pressurized exponential assembly TZ. By R. Persson, A. J. W. Andersson and C-E. Wikdahl. 1966. 56 p. Sw. cr. 8:–.

255. Decontamination experiments on intact pig skin contaminated with beta-gamma-emitting nuclides. By K. A. Edwardsson, S. Hagsgård and Å. Swensson. 1966. 35 p. Sw. cr. 8:–.

256. Pertubation method of analysis applied to substitution measurements of buckling. By R. Persson. 1966. 57 p. Sw. cr. 8:–.

257. The Dancoff correction in square and hexagonal lattices. By I. Carlvik. 1966. 35 p. Sw. cr. 8:–.

258. Hall effect influence on a highly conducting fluid. By E. A. Witalis. 1966. 13 p. Sw. cr. 8:–.

259. Analysis of the quasi-elastic scattering of neutrons in hydrogenous liquids. By S. N. Purohit. 1966. 26 p. Sw. cr. 8:–.

260. High temperature tensile properties of unirradiated and neutron irradiated 20Cr–35Ni austenitic steel. By R. B. Roy and B. Solly. 1966. 25 p. Sw. cr. 8:–.

261. On the attenuation of neutrons and photos in a duct filled with a helical plug. By E. Aalto and Å. Krell. 1966. 24 p. Sw. cr. 8:–.

262. Design and analysis of the power control system of the fast zero energy reactor FR-0. By N. J. H. Schuch. 1966. 70 p. Sw. cr. 8:–.

263. Possible deformed states in ^{115}In and ^{117}In. By A. Bäcklin, B. Fogelberg and S. G. Malmskog. 1967. 39 p. Sw. cr. 10:–.

264. Decay of the 16.3 min. ^{182}Ta isomer. By M. Höjeberg and S. G. Malmskog. 1967. 13 p. Sw. cr. 10:–.

265. Decay properties of ^{147}Nd. By A. Bäcklin and S. G. Malmskog. 1967. 15 p. Sw. cr. 10:–.

266. The half life of the 53 keV level in ^{197}Pt. By S. G. Malmskog. 1967. 10 p. Sw. cr. 10:–.

267. Burn-up determination by high resolution gamma spectrometry: Axial and diametral scanning experiments. By R. S. Forsyth, W. H. Blackladder and N. Ronqvist. 1967. 18 p. Sw. cr. 10:–.

268. On the properties of the $s_{1/2} \longrightarrow d_{3/2}$ transition in ^{199}Au. By A. Bäcklin and S. G. Malmskog. 1967. 23 p. Sw. cr. 10:–.

269. Experimental equipment for physics studies in the Ågesta reactor. By G. Bernander, P. E. Blomberg and P.-O. Dubois. 1967. 35 p. Sw. cr. 10:–.

270. An optical model study of neutrons elastically scattered by iron, nickel, cobalt, copper, and indium in the energy region 1.5 to 7.0 MeV. By B. Holmqvist and T. Wiedling. 1967. 20 p. Sw. cr. 10:–.

271. Improvement of reactor fuel element heat transfer by surface roughness. By B. Kjellström and A. E. Larsson. 1967. 94 p. Sw. cr. 10:–.

272. Burn-up determination by high resolution gamma spectrometry: Fission product migration studies. By R. S. Forsyth, W. H. Blackadder and N. Ronqvist. 1967. 19 p. Sw. cr. 10:–.

273. Monoenergetic critical parameters and decay constants for small spheres and thin slabs. By I. Carlvik. 24 p. Sw. cr. 10:–.

274. Scattering of neutrons by an anharmonic crystal. By T. Högberg, L. Bohlin and I. Ebbsjö. 1967. 38 p. Sw. cr. 10:–.

275. The $|\Delta K| = 1$, E1 transitions in odd-A isotopes of Tb and Eu. By S. G. Malmskog, A. Marelius and S. Wahlborn. 1967. 24 p. Sw. cr. 10:–.

276. A burnout correlation for flow of boiling water in vertical rod bundles. By Kurt M. Becker. 1967. 102 p. Sw. cr. 10:–.

277. Epithermal and thermal spectrum indices in heavy water lattices. By E. K. Sokolowski and A. Jonsson. 1967. 44 p. Sw. cr. 10:–.

278. On the $d_{5/2} \leftrightarrow g_{7/2}$ transitions in odd mass Pm nuclei. By A. Bäcklin and S. G. Malmskog. 1967. 14 p. Sw. cr. 10:–.

279. Calculations of neutron flux distributions by means of integral transport methods. By I. Carlvik. 1967. 94 p. Sw. cr. 10:–.

280. On the magnetic properties of the K=1 rotational band in ^{188}Re. By S. G. Malmskog and M. Höjeberg. 1967. 18 p. Sw. cr. 10:–.

281. Collision probabilities for finite cylinders and cuboids. By I. Carlvik. 1967. 28 p. Sw. cr. 10:–.

282. Polarized elastic fast-neutron scattering of ^{12}C in the lower MeV-range. I. Experimental part. By O. Aspelund. 1967. 50 p. Sw. cr. 10:–.

283. Progress report 1966. Nuclear chemistry. 1967. 26 p. Sw. cr. 10:–.

284. Finite-geometry and polarized multiple-scattering corrections of experimental fast-neutron polarization data by means of Monte Carlo methods. By O. Aspelund and B. Gustafsson. 1967. 60 p. Sw. cr. 10:–.

285. Power disturbances close to hydrodynamic instability in natural circulation two-phase flow. By R. P. Mathisen and O. Eklind. 1967. 34 p. Sw. cr. 10:–.

286. Calculation of steam volume fraction in subcooled boiling. By S. Z. Rouhani. 1967. 26. p. Sw. cr. 10:–.

287. Absolute E1, $\Delta K = 0$ transition rates in odd-mass Pm and Eu-isotopes. By S. G. Malmskog. 1967. 33 p. Sw. cr. 10:–.

288. Irradiation effects in Fortiweld steel containing different boron isotopes. By M. Grounes. 1967. 21 p. Sw. cr. 10:–.

289. Measurements of the reactivity properties of the Ågesta nuclear power reactor at zero power. By G. Bernander. 1967. 43 p. Sw. cr. 10:–.

290. Determination of mercury in aqueous samples by means of neutron activation analysis with an account of flux disturbances. By D. Brune and K. Jirlow. 1967. 15 p. Sw. cr. 10:–.

291. Separtaion of ^{51}Cr by means of the Szilard-Chalmers effect from potassium chromate irradiated at low temperature. By D. Brune. 1967. 15 p. Sw. cr. 10:–.

292. Total and differential efficiencies for a circular detector viewing a circular radiator of finite thickness. By A. Lauber and B. Tollander. 1967. 45 p. Sw. cr. 10:–.

293. Absolute M1 and E2 transition probabilities in ^{233}U. By S. G. Malmskog and M. Höjeberg. 1967. 37 p. Sw. cr. 10:–.

Förteckning över publiserade AES-rapporter

1. Analys medelst gamma-spektrometri. Av D. Brune. 1961. 10 s. Kr 6:–.
2. Bestrålningsförändringar och neutronatmosfär i reaktortrycktankar – några synpunkter. Av M. Grounes. 1962. 33 s. Kr 6:–.
3. Studium av sträckgränsen i mjukt stål. Av G. Östberg och R. Attermo 1963. 17 s. Kr 6:–.
4. Teknisk upphandling inom reaktorområdet. Av Erik Jonson. 1963. 64 s. Kr 8:–.
5. Ågesta Kraftvärmeverk. Sammanställning av tekniska data, beskrivningar m. m. för reaktordelen. Av B. Lilliehöök. 1964. 336 s. Kr 15:–.
6. Atomdagen 1965. Sammanställning av föredrag och diskussioner. Av S. Sandström. 1965. 321 s. Kr 15:–.

Additional copies avaiable at the library of AB Atomenergi, Studsvik, Nyköping, Sweden. Micronegatives of the reports are obtainable through Filmprodukter, Gamla landsvägen 4, Ektorp, Sweden.

EOS-tryckerierna, Stockholm 1967